POWER ELECTRONICS ASSISTED VOLTAGE REGULATORS FOR MODERN DISTRIBUTION SYSTEMS

by

Yafeng Wang

A dissertation submitted to the faculty of
The University of North Carolina at Charlotte
in partial fulfillment of the requirements
for the degree of Doctor of Philosophy in
Electrical Engineering

Charlotte

2021

Approved by:

____
Dr. Tiefu Zhao

____
Dr. Madhav Manjrekar

____
Dr. Babak Parkhideh

____
Dr. Maciej Noras

ABSTRACT

YAFENG WANG. Power Electronics Assisted Voltage Regulators for Modern Distribution Systems. (Under the direction of DR. TIEFU ZHAO)

Step voltage regulator (SVR) has been utilized in power distribution systems for decades. The induced arc from the conventional SVR tap change and the voltage instability from the renewable energy penetration impose constraints on the conventional SVRs' lifetime. With more distributed power generation and renewable energy penetration, voltage fluctuation and power generation variation can be observed more frequently in the modern power distribution network. More tap change operations are required for SVR to regulate the line voltage. However, the tap changing mechanism of the conventional SVR always generates an electric arc when tap changes, which imposes constraints on conventional SVRs, such as lifetime and maintenance period. Meanwhile, the voltage regulation accuracy cannot be guaranteed since the SVR regulates the voltage step by step. The power electronics transformer solution was proposed but requires the power converter capacity proportional to the voltage regulation range, which significantly increases the system cost.

Motivated by the issues mentioned above, several PE-assisted arcless tap change topologies are proposed to reduce the contact erosion rate of tap changers in SVR. The system efficiency is the same with the conventional SVR in normal operation, while the converter power rating is only 0.3% of the total system power, which also reduces the system cost compared with the full power electronics solutions. Based on the proposed arcless tap change mechanism, a hybrid voltage regulator is proposed. Stepless load voltage

regulation is achieved while the tap changer mechanism remains in the system, which helps to promote the upgrade to the existing power distribution systems.

A scaled-down prototype of the arcless SVR is developed to verify the proposed arcless tap changing method. The hardware test results verified the proposed arcless step voltage regulator can eliminate arcing during the tap change and reduce the contact erosion rate by over 10,000 times the conventional arcing SVR. Other advantages of the novel method over the conventional SVR, such as advanced load voltage regulation and volt/var control, are also verified. The proposed hybrid voltage regulator was simulated and experimentally validated. The experimental results demonstrate arcless tap change operation, stepless voltage regulation, and load voltage continuity during the tap change.

For PE-based hybrid voltage regulators, many functions, such as fast voltage regulation, flicker compensation, and var control, can be accomplished, which cannot be achieved from the conventional SVR. This research also proposed a new topology of the hybrid voltage regulation transformer (VRT). The feasibility and capability of var control are investigated for different load power factors and input voltage percentage when the voltage regulation does not exceed the power converter capacity. The simulation results illustrate the feasibility of implementing var control while the load voltage is being regulated.

This dissertation also proposed a new hybrid transformer based on interline power converters for voltage regulation. The maximum power delivered by converters is reduced in half compared with the conventional series compensation configuration for the same voltage regulation range. Therefore, the proposed hybrid transformer exhibits a higher overall efficiency covering a wide range of voltage regulation. Comparison between the conventional series voltage compensation method and the proposed interline power converter-based method is presented based on the operation principle, the converter power, and the overall system efficiency.

ACKNOWLEDGEMENTS

I would like to thank my academic advisor, Dr. Tiefu Zhao for his guidance and supervision on my research and Ph.D. study. His professional experience and patient instructions have been encouraging me through my Ph.D. career at UNC Charlotte. Dr. Zhao's dedication to his research group and insightful scope of my personal development impressed me significantly and made me confident in my daily study and research work.

I would also like to express my greatest gratitude to my Doctoral Dissertation Committee members, Dr. Madhav Manjrekar and Dr. Babak Parkhideh, and my graduate faculty representative, Dr. Maciej Noras for their constructive suggestions and help for my dissertation. My colleagues and group members, Luocheng Wang, Xiwen Xu, Haichen Liu, Shangze Chen and Kamal Paul, from Renewable Energy and Power Electronics Advanced Research Lab (RE-PEARL) have also been of so much help and support.

I also want to express my sincere appreciation for GASP grant from UNC Charlotte for my Ph.D. tuition fund and the project collaboration and financial support from Eaton Corporation for my research projects.

Last but not the least, I would like to appreciate my wife and all my family members for their understanding and support throughout my Ph.D. journey.

DEDICATION

I dedicate my dissertation to my wife, Mrs. Shengnan Ju, whose love is the greatest gift of my life and whose commitment, support, and devotion are encouragement and power for the journey of my Ph.D. study; and my parents, Mr. Weihong Wang and Mrs. Hongxia Wang, who introduced me to this fascinating world and who have always been a continual source of pride and enlightenment of my life.

TABLE OF CONTENTS

LIST OF TABLES

LIST OF FIGURES

LIST OF ABBREVIATIONS

UNCC	University of North Carolina at Charlotte
ECE	Electrical and Computer Engineering
RE-PEARL	Renewable Energy and Power Electronics Advanced Research Lab
PE	Power Electronics

CHAPTER 1: INTRODUCTION

1.1 Background of Conventional Step Voltage Regulator

Step voltage regulators are widely applied to the distribution systems to compensate for the voltage drop across the power lines and other types of voltage variations. The conventional SVR is an autotransformer-based structure [1]. Conventional SVRs usually have 9 taps and 10% voltage regulation range and the configuration in Fig. 1.1 has been employed in the distribution systems for decades. The preventive transformer, also known as the bridging reactor, limits the circulating current when the two contacts are at different positions. The equalizer windings are coupled with the main transformer to reduce the tap changer interruption duty. The voltage regulation is conducted by moving taps up and down to adjust the transformer turns ratio, as a result, to regulate the load-side voltage within the limit.

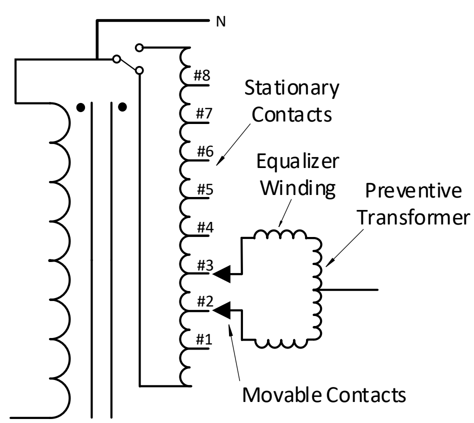

Figure 1.1 Conventional step voltage regulator

1.2 Issues with Conventional Step Voltage Regulator

For the conventional SVRs, electric arc can be frequently observed when the contact separates from an energized tap in the conventional SVR configuration. In the tap changing process, electric arc often occurs between metal contacts when they separate from the energized contacts and large current is cut off. Carbide accumulation and transformer oil degradation are also speeded up due to the frequent arc. Contact erosion and transformer oil degradation result due to the frequent arc which can be detected and measured [2-3]. Induced maintenance leads to unpredictable system shutdown and capital loss.

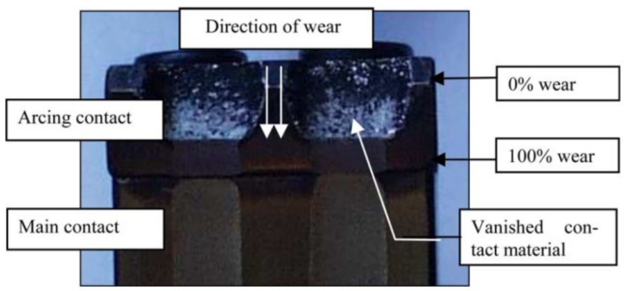

Figure 1.2 Worn arcing contacts taken from an aged On-Load Tap Changer (OLTC) [3]

Another disadvantage of the conventional SVR is that the voltage is regulated step by step, hence accurate and fast voltage regulation cannot be acquired between each step. The tap change operation interval of the conventional SVR could be several minutes. And the mechanical tap change movement speed is restricted by the tap changer mechanism.

1.3 Modern Distribution Systems Pattern Impacts on SVRs

More and more renewable energy generation facilities have been incorporated into the modern power system during the last two decades, such as wind, solar and hydropower. Renewable energy resources, as distributed energy resources (DERs), are highly distributed, which heavily depends on the geological positions and local climate. The instability of distributed power generation brings more voltage fluctuation and power generation variation to the regional transmission systems due to the variable weather and other unpredictable conditions. Studies in [4] and [5] show that both voltage fluctuation and excessive transformer tap changes result from the induced fluctuations in photovoltaic (PV) power. The phenomena become more severe under the high PV penetration condition. Figure 1.3 shows an example of PV penetration impact on conventional tap changer operations of SVRs.

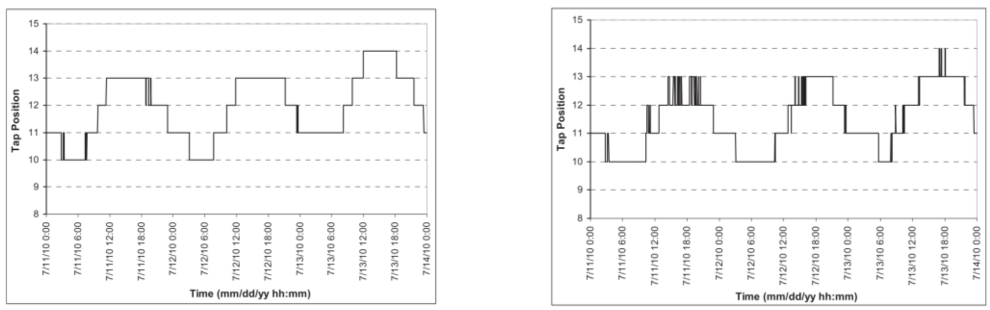

Figure 1.3 Substation transformer tap changer position without PV (left) and with PV (right) [4]

Another noticeable challenge is the increasing number of plug-in electric vehicles (PEVs) which is a group of random and unpredictable loads in the modern power system. Reference [6] addresses that PEV charging could decrease distribution transformer life by 93% where the impact of transient ambient temperature is not considered. There is no doubt that the increasing number of random PEVs charging brings uncertainty as the load changes. Voltage fluctuation can be caused by sudden and frequent load change as well. Based on the above facts, SVRs contact erosion is further accelerated because of the frequent arc erosion.

1.4 Technology Roadmap of the Proposed Research

Based on the existing technologies, many advanced PE-based solutions can be implemented to mitigate the issues from conventional SVRs. The full PE voltage regulator, such as Solid State Transformer (SST), has more functionalities, such as fast voltage regulation, var control and voltage sag/swell compensation but the system efficiency will be lower than conventional SVRs and costly due to the full rating of PE converter. Hybrid Voltage Regulator (HVR), as an intermediate solution between conventional SVR and SST, is a cost-efficient solution with a fractionally rated PE converter that can achieve arcless tap change and accurate voltage regulation. With most components remained in the system, HVR just needs a simple upgrade based on the conventional SVR as a retrofit with high efficiency. Considering the great number of conventional SVRs that have already been implemented in the existing distribution systems for decades, HVR can be easily promoted into modern power distribution systems. Based on these facts, a technology roadmap of the proposed research is proposed as shown in Figure 1.4.

The dissertation focuses on the development of HVR firstly to solve the arcless tap change issue. Then, a hybrid PE solution with stepless and accurate voltage regulation is investigated to achieve better performance compared with conventional SVRs. In the future, our research scope is the full PE solid-state transformer with the full range of fast voltage

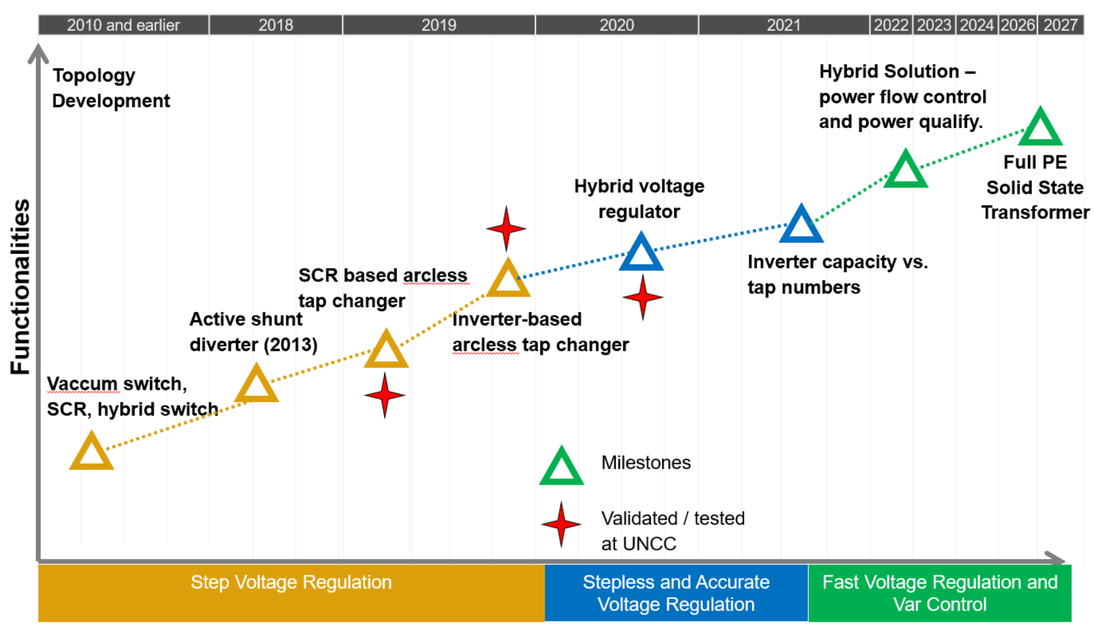

Figure 1.4 Technology roadmap of the proposed research

regulation and var control capability. With the expected lower price and higher efficiency of semiconductor devices applied to SST, the voltage regulator system cost and efficiency are expected to be comparable to the conventional SVR.

1.5 Dissertation Organization

Chapter 2 presents the literature review on the existing technologies to mitigate voltage regulator aging and PE-assisted voltage regulation methods. In Chapter 3, two types of proposed arcless tap change solutions are introduced and validated by both simulation and prototype tests. In Chapter 4, a hybrid voltage regulator is proposed to achieve both arcless tap change operation and stepless voltage regulation and simulation results and prototype test results are also presented. In Chapter 5, a series-connected voltage regulator is investigated for the var control capability. Chapter 6 summarized the publications and conclusion of the dissertation.

CHAPTER 2: LITERATURE REVIEW ON EXISTING TECHNOLOGIES

2.1 Existing Methods Based on Power System Planning and Control

Step voltage regulator erosion and distribution transformer aging exist widely in power distribution systems. Power system operation control can be optimized to reduce the tap change operation times in a given period to adapt to different voltage regulation patterns. [7] - [10] proposed methods of electric vehicle smart charging and location planning to mitigate the voltage problem in the distribution system with high PV penetration. Study in [11] demonstrates Volt-Var optimization in the distribution system to extend the lifetime of distribution transformers. Similarly, reference [12] presents the reactive power control method for the parallel operation of transformers in distribution systems with PV penetration. An adaptive method of upgrading different voltage control strategies based on different PV penetration rates is proposed in [13].

2.2 Existing Arcless Tap Change Methods

Even though the voltage problem due to the variation of power generation and consumption can be partially relieved by power system control and planning, a centralized solution to eliminate the arc of each tap change is still fundamental from the power electronics perspective. Advantages of arcless voltage regulators are discussed in [14]. Vacuum switches have been utilized for many years in most of the high current circuit breakers and can be implemented for arc elimination of tap changes [15]. But the large space requirement and high material cost for one or more vacuum interrupters and associated mechanisms make it difficult for commercial deployment.

Semiconductors have been widely developed in recent years and exhibit better switching performance to cut off current without arcing. Several configurations are proposed, such as anti-paralleled SCRs and solid-state bidirectional switches [16]-[20]. However, the steady-state conduction loss of the semiconductor devices is significantly higher than the metal conductors. Commercial substations and distribution systems cannot afford voltage regulators with poor efficiency. For this reason, the idea of hybrid switches is proposed in [21] and [22] to lower the conduction loss. Additional snubber circuits are required to deal with hard switching of the semiconductor devices. The current redirection method is proposed in [23] to prevent the energized contact separation. In this way, the arc can be eliminated when the branch current is controlled to zero before the mechanical tap change.

2.3 Existing PE-Assisted Voltage Regulation Methods

[24] and [25] use AC choppers or direct AC-AC converters to regulate the voltage. The mechanical switches and taps are completely excluded in these topologies. Harmonics generated by high-frequency switching need additional passive or active filter design and are not suitable for applications with high power quality requirements. Power electronics transformer is proposed in [26], [27] and [28] to compensate the load voltage fluctuation, which can be accurate and continuous, through full-rated power electronics converter or hybrid AC/AC solutions. Fig. 2.1 shows the general hybrid distribution transformer topology.

However, the voltage regulation range is proportional to the inverter capacity which is directly related to the system cost. For example, a hybrid distribution transformer of 10% voltage regulation range requires the converter capacity to be 10% of the distribution transformer power rating. Although solid-state transformers are a great candidate for the voltage regulator in the next-generation distribution system, they still suffer from the poor system peak efficiency of 97% and the conventional low-frequency transformer efficiency can easily reach beyond 99% [29]-[31].

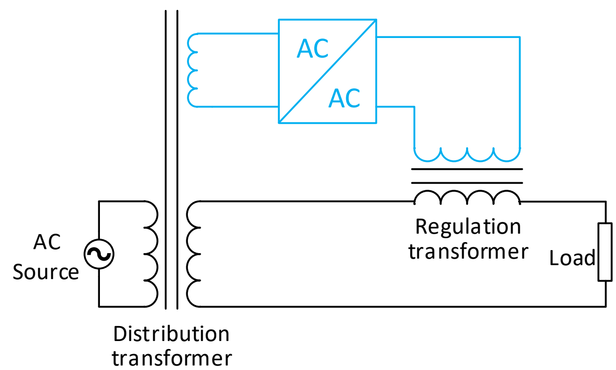

Figure 2.1 Hybrid distribution transformer

Voltage regulation is necessary from portable electronic devices to the power distribution systems to maintain the voltage magnitude. In recent years, voltage variation can be observed more frequently due to renewable energy penetration and the power generation variation from distributed energy resources (DERs). Dynamic voltage restorer (DVR) at medium voltage level is discussed in [32] to compensate voltage sags as a cost-friendly solution. And studies in [33]-[35] proposed other DVR functions, such as selective harmonic compensation and fault current limiting. The configuration of DVR is shown in Fig. 2.2. The DC side of the inverter usually consists of batteries, super-capacitors, or other types of energy storage systems. Therefore, the DVRs are usually utilized to compensate voltage deviation for a short time. In [36], DVR is integrated with distribution transformer to achieve step-less voltage regulation, but the regulation speed is still limited by the tap

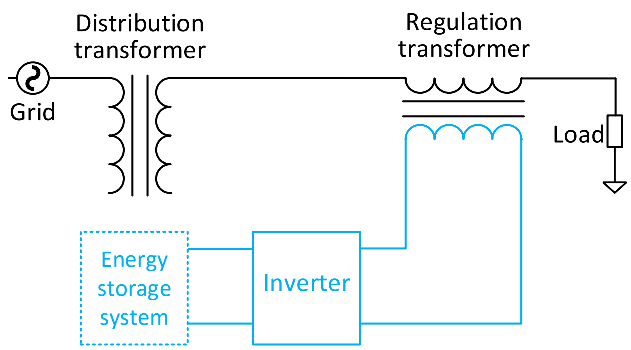

Figure 2.2 Dynamic voltage restorer (DVR)

changer mechanism. The static synchronous compensator (STATCOM) is integrated with distribution transformer in [37] and [38] for the reactive power compensation with a cost-effective method. The smart transformer with full power electronics solution in [27] is rated at the feeder's full power, which is not cost-friendly compared to the previous hybrid solutions [36]-[38]. Study in [39] discusses the var control considerations for the hybrid distribution transformer. But var control capabilities and limits are not investigated when the voltage magnitude regulation is implemented and takes part in the converter capacity.

CHAPTER 3: PROPOSED PE-ASSISTED ARCLESS TAP CHANGE

3.1 Circuit Configuration

3.1.1 Arcless Step Voltage Regulator Based on Series-Connected Converter

For the arcless tap change operation, two topologies are proposed based on the conventional SVR. Series-connected and paralleled PE converters are able to assist the arcless tap change operation. The proposed series-connected arcless step voltage regulator, as shown in Fig. 3.1, includes the main transformer, equalizer, bias transformer, and back-to-back converter. Both the shunt winding and the equalizer windings are on the same magnetic circuit with the main transformer windings. The shunt winding provides the voltage source for the power converter. The equalizer windings are connected in series in the branch loop to balance the loading conditions of the power converter in the bridging and non-bridging positions. The power converter generates a bias current through the bias transformer to overcome the voltage difference between the two taps where the two branches are connected. The net result of this bias current is to reduce one branch current to zero current and the entire load current effectively flowing through the other branch. Arcless tap changing is achieved by suppressing the target branch current to zero before

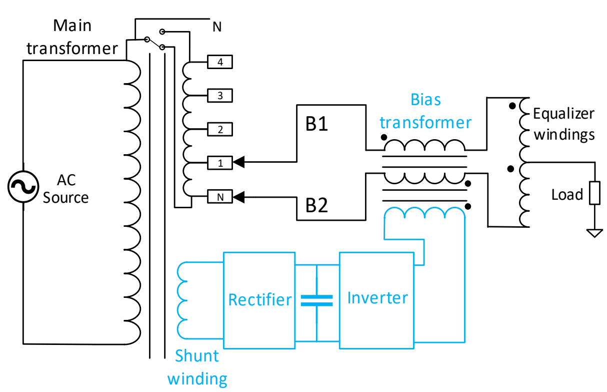

Figure 3.1 Proposed arcless step voltage regulator based on series-connected converter

the actual mechanical tap change. Therefore, the electric arc can be eliminated when tap changes.

Fig. 3.2 illustrates two different tap contact positions. The two branch contacts are on the adjacent taps separately at the bridging position. And the non-bridging position is where two branch contacts are on the same tap.

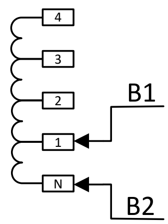

Figure 3.2 Bridging position (left) and non-bridging position (right)

The equivalent circuits of the two branches are shown in Fig. 3.3.

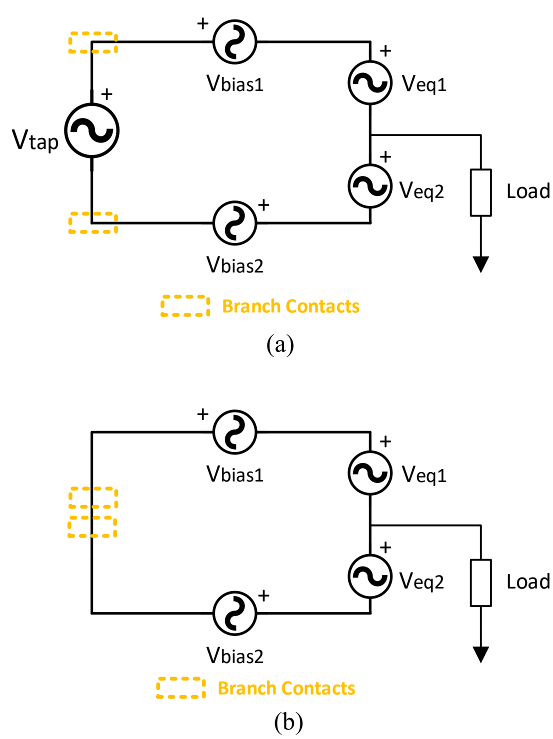

Figure 3.3 (a) Bridging position equivalent circuit, (b) Non-bridging position equivalent circuit

The relationship between V_{tap}, V_{eq1}, and V_{eq2} are represented by equation (1-3) and they are determined by the transformer winding turns ratio. V_{tap} is the tap winding voltage between each adjacent tap. V_{bias1} and V_{bias2} are the two secondary windings voltage of the bias transformer. V_{eq1} and V_{eq2} are the voltage of the two equalizer windings which are coupled with the main transformer core. To suppress the upper branch current, as an example, the injected bias transformer voltage should meet equation (4) for the bridging position. For the non-bridging position, the polarity of the bias transformer voltage should be reversed as equation (5). The equations are derived when the windings leakage inductance and the induced voltages are negligible compared to the major tap voltage difference. More specified model analysis is provided in Section 3.2.

$$V_{eq1} = V_{eq2} = \frac{1}{4}V_{tap} \tag{1}$$

$$V_{bias1} = V_{bias2} \tag{2}$$

$$V_{eq1} + V_{eq2} = 0.5V_{tap} \tag{3}$$

$$V_{bias1} + V_{bias2} = 0.5V_{tap} \tag{4}$$

$$V_{bias1} + V_{bias2} = -(0.5V_{tap}) \tag{5}$$

3.1.2 Arcless Step Voltage Regulator based on Paralleled PE Converter

The proposed arcless voltage regulator based on paralleled PE converter, as shown in Fig. 3.4, consists of the main transformer, shunt windings, equalizer windings, back-to-back converter and preventive transformer. The shunt windings and the equalizer windings are coupled with the same core of the main transformer. The back-to-back converter generates a voltage to balance the voltage difference between the two taps and provides an additional current path hence to reduce the current flowing through one of the branches to zero before the contacts separate. Then, the arcing can be eliminated when tap moves apart from the metal contacts.

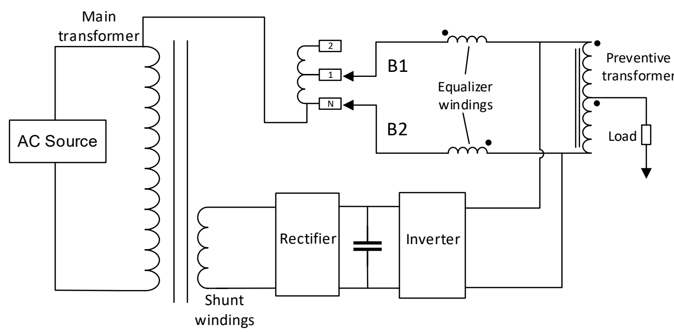

Figure 3.4 Proposed arcless step voltage regulator based on paralleled PE converters

3.2 Tap Change Operation Principle and Sequence

Since the power electronics converter does not need to operate during the SVR normal operation time and only works when one tap or multiple tap changes are required, the transient performance is one of the most important metrics to evaluate the arcless tap changing operation. The time needed to suppress the branch current and how the converter adapts to different tap positions to maintain the current suppression will all affect the voltage regulation performance of the distribution system.

For the series-connected arcless SVR solution, a typical tap lowering operation is shown in Fig. 3.5. Two branches are previously on tap N and tap 1. Upper branch current *I_B1* is suppressed to zero and then the upper branch moves from tap 1 to tap N. The detail of the tap changing operation in Fig. 3.5 is:

(a) Tap branches are in bridging position and B1 and B2 share the load current equally. DC bus is pre-charged by the rectifier and able to achieve the volt/var control if necessary. The inverter is disabled, so the bias transformer acts as the preventive transformer to limit the circulating current in the branch loop.

(b) Inverter starts to work. The upper branch current *I_B1* is suppressed to zero after a few cycles while the load current completely flows through the lower branch. Tap change command can be given after the current suppression is confirmed.

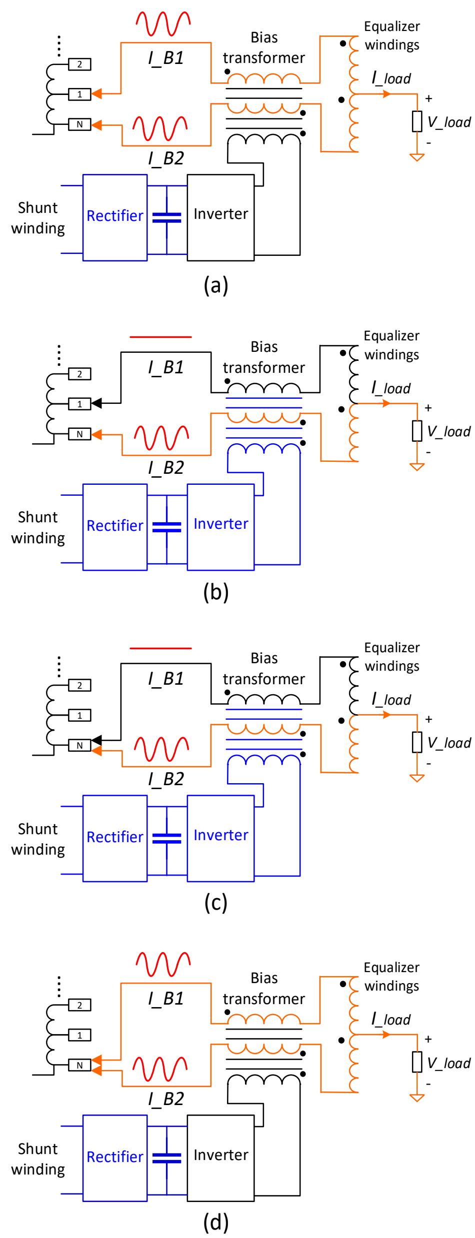

Figure 3.5 Circuit operations by time sequence

(c) The upper branch contact starts moving away from the original tap 1 without arcing and connects to the tap N. The upper branch current is still regulated to zero to avoid the electric arc due to the mechanical bounce from the metal contact connection.

(d) The inverter is shut down and stops suppressing the upper branch current. B1 and B2 share the load current again at the new position. During the whole tap changing process, the rectifier keeps working to regulate the DC bus voltage.

For the paralleled converter-based arcless SVR solution, A tap changing operation sequence is proposed to ensure the arcless operation with the assist of power converters. Fig. 3.6 illustrates the proposed tap changing sequence from bridging position (taps at position #1 and N) to non-bridging position (taps all at position N). The tap changing operation sequence is described below.

(a) Tap branches are in bridging position and B1 and B2 share the load current. DC bus is pre-charged by the rectifier while the inverter gate signals are disabled, so there is no current flowing through the inverter. No voltage is injected into the branch loop.

(b) The inverter gate signals are enabled and the inverter starts to work. Upper branch current I_B1 is suppressed to zero. All of the load current flows through tap N and lower branch. Due to the current balancing function of the preventive transformer, the load current is divided into two equal currents flowing through the upper and lower parts of the preventive transformer. The dividing point is the inverter connection point of the lower branch, so the inverter current is half of the load current.

(c) The upper branch contact starts moving away from tap #1 without arcing and connects to tap N. Upper branch current is still regulated to zero after tap change, so there is no arcing during the whole tap change process.

(d) The inverter is shut down and stops suppressing upper branch current, B1 and B2 share the load current equally again at the non-bridging position.

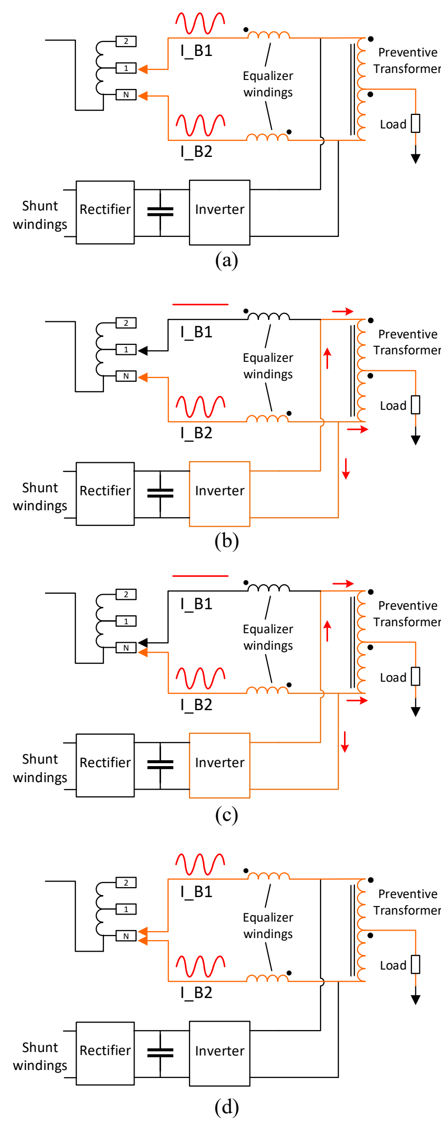

Figure 3.6 Arcless tap change operations by time sequence

The operation of arcless tap change is achieved by suppressing the target branch current to zero before and after the mechanical tap change, so that there is no arcing when the metal contacts separate and connect.

3.3 Control Stratety and Model Analysis

For the series-connected converter solution, the rectifier can hold the DC bus voltage and compensate the reactive power for the main transformer and the rectifier control algorithm is shown in Fig. 3.7. Var control can be achieved by adjusting the *Iq_ref* in the rectifier control to obtain unity power flow from the source side if the converter capacity permits.

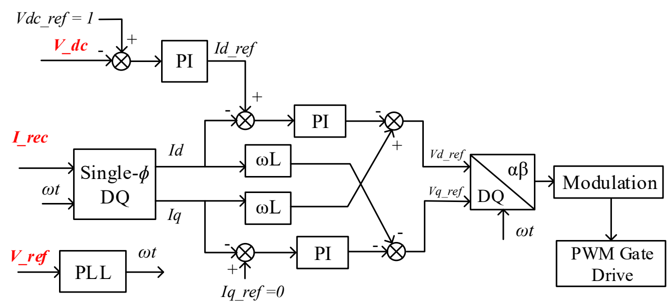

Figure 3.7 Rectifier control (*I_rec*: rectifier input current, *V_ref*: load voltage, *V_dc*: DC bus voltage)

The inverter control block diagram is shown in Fig. 3.8 and the target of the inverter output control is to suppress the upper or lower branch current to zero. Rectifier and inverter are both H-bridge configuration.

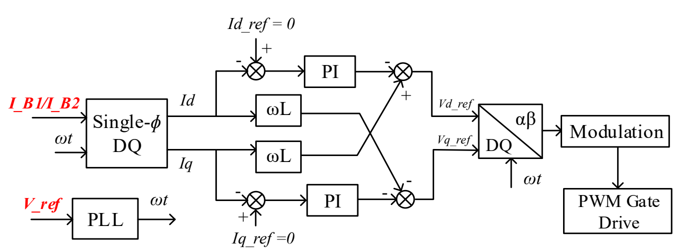

Figure 3.8 Inverter control (I_B1/I_B2: upper/lower branch current, V_ref: load voltage)

Although the branch current can be suppressed to zero for one tap position, the voltage difference between the bridging position and non-bridging position after the tap change still requires the inverter output voltage to be reversed according to equation (4) and (5). Before and after the tap change, the inverter output voltage needed to suppress the target branch current must be analyzed more specifically. A more specified circuit model is presented in Fig. 3.9 as the leakage inductance of all the windings are considered. Resistance in these short sections of conductor winding is estimated to be small enough to neglect.

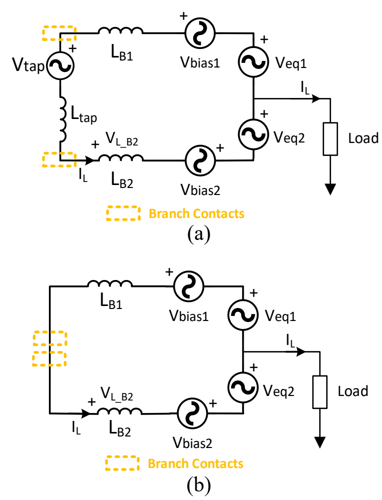

Figure 3.9 (a) Bridging position equivalent circuit, (b) Non-bridging position equivalent circuit

L_{B1} and L_{B2} represent the upper branch and lower branch leakage inductance respectively. L_{tap} is the tap winding leakage inductance between each adjacent tap. Now that the upper branch current is already suppressed to zero before the mechanical tap change movement, all the load current flows directly to the load through the lower branch. For this reason, only the induced voltage on the lower branch leakage inductance, which is V_{L_B2}, is taken into consideration as the tap position changes. And the induced voltage V_{L_B2} is 90 degree leading to the load current.

Vector analysis is shown in Fig. 3.10 for different tap positions and power factor (PF). V_s and V_{eq} are source voltage and equalizer windings voltage respectively and both of them are in phase with each other since they are coupled with the same magnetic core. V_{inv} is the inverter output voltage. I_L is the load current. For better analysis, V_{inv} can be decomposed into V_{inv_S} and V_{inv_IL}. V_{inv_S} is to balance the voltages in the branch loop that are in phase with the source voltage, such as V_{tap} and V_{eq}. V_{inv_IL} is to balance the induced voltage on the leakage inductance, which can be represented by equation (6), but it is still quite smaller than V_{inv_S}. α is the angle between V_{inv} and V_{inv_S}. β is the angle between V_{inv_IL} and the d axis. It can be noticed that V_{inv_IL} does not change when the tap position changes since V_{inv_IL} is always perpendicular to the load current I_L when circuit resistance is neglected. The bias transformer turns ratio is 4:1:1 for the inverter output side winding and the series-connected bias windings in the branches. But the equivalent inverter output voltage that works in the branch loop is the sum of both bias winding voltage, so the relationship of the equivalent inverter output voltage is defined as equation (7). Equation (8) and (9) define the V_{inv_S} in the bridging and non-bridging positions. Therefore, the inverter output voltage component on the d axis can be derived as equation (10) and (11) for the bridging and non-bridging position respectively. However, the V_{inv} component on the q axis, as represented by equation (12), does

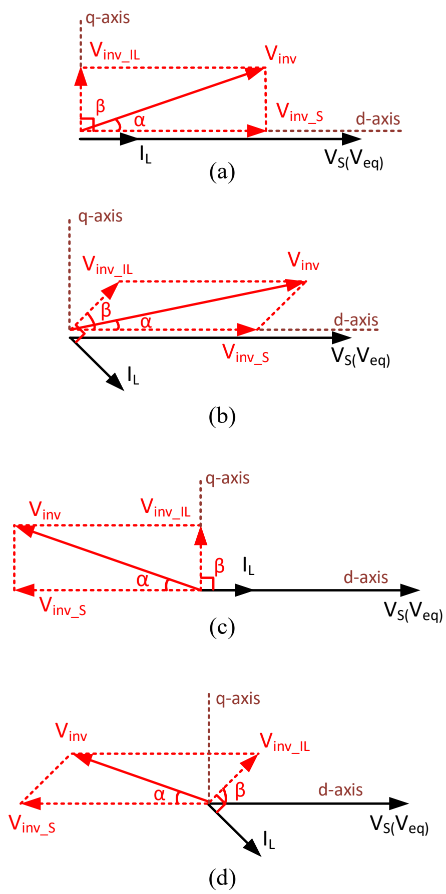

Figure 3.10 Vector diagram of the bridging position: (a) PF = 1, (b) PF <1 and the non-bridging position: (c) PF = 1, (d) PF < 1

not change after the tap change. As a result, the only difference in the inverter output voltage between the bridging and non-bridging positions is the difference between V_{d1} and V_{d2}. The inverter output voltage change on the d axis is always a fixed difference no matter what the load power factor is. And its component on the q axis stays the same after the tap change.

$$V_{inv\_IL} = j\omega L_{B2} I_L \tag{6}$$

$$V_{inv} = V_{bias1} + V_{bias2} \tag{7}$$

$$V_{inv\_s} = V_{tap} - V_{eq1} - V_{eq2} = 0.5V_{tap} \tag{8}$$

$$V_{inv\_s} = -V_{eq1} - V_{eq2} = -0.5V_{tap} \tag{9}$$

$$V_{d1} = |V_{inv\_s}| + |V_{inv\_IL}| cos\beta > 0 \tag{10}$$

$$V_{d2} = -|V_{inv_s}| + |V_{inv_{IL}}| cos\beta < 0 \tag{11}$$

$$V_q = |V_{inv\_IL}| sin\beta > 0 \tag{12}$$

This finding shows a simple way of adapting the inverter or the controller to the next status of the tap position, which is adding a compensation signal directly on the controller *Vd_ref* output during the mechanical tap change. The mechanical movement also provides the time window to implement the compensation in the control algorithm. Hence, an improved inverter control is developed as Fig. 3.11. A step compensation signal is added to the *Vd_ref* signal of the inverter control.

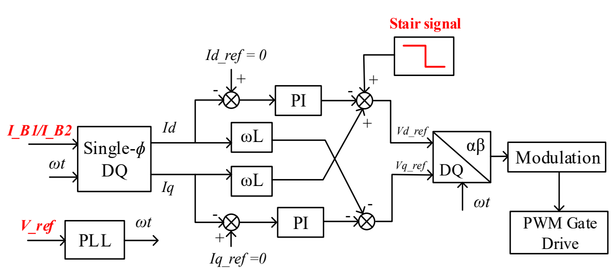

Figure 3.11 Improved inverter control

For the paralleled converter solution, the equivalent circuits of the two branches are shown in Fig. 3.12. The bridging position is where the two branch contacts are on the adjacent taps separately. The non-bridging position is where two branch contacts are on the same tap. V_{tap} stands for the tapped winding voltage. V_{prev1} and V_{prev2} are the two voltages of the preventive transformer windings, which are induced while the preventive transformer acts as a mutual inductance to suppress the circulating current in the loop. V_{eq1} and V_{eq2} are the voltage of the two equalizer windings which are coupled with the main transformer core. The relationship between V_{tap}, V_{eq1} and V_{eq2} are determined by the windings turns ratio, as represented by equation (13-15). To suppress the upper branch current, for example, the injected inverter output voltage should meet the equation (16) for the bridging position. For the non-bridging position, the polarity of the inverter output voltage should be reversed as equation (17). The required inverter output voltage for the

$$V_{eq1} = V_{eq2} \tag{13}$$

$$V_{prev1} = V_{prev2} \tag{14}$$

$$V_{eq1} + V_{eq2} = 0.5V_{tap} \tag{15}$$

$$V_{inv} = V_{prev1} + V_{prev2} = 0.5V_{tap} \tag{16}$$

$$V_{inv} = -(V_{eq1} + V_{eq2}) \tag{17}$$

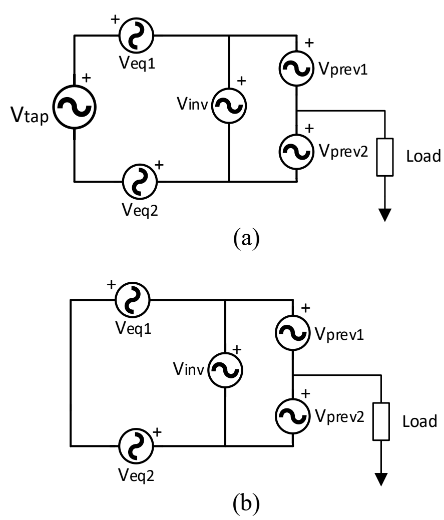

Figure 3.12 Equivalent circuit: (a) bridging position, (b) non-bridging position

bridging and non-bridging positions are opposite and the magnitude is half of the tap voltage.

The rectifier and inverter control block diagrams are shown in Fig. 3.13 and Fig. 3.14. The rectifier can regulate the DC bus voltage and realize Var control for the main transformer. The inverter controls the output voltage to suppress the upper or lower branch current to zero. Rectifier and inverter are both H-bridge configuration. The step compensation strategy mentioned previously in the series-connected configuration also applies to the paralleled converter configuration for the contact making current suppression after the mechanical tap change.

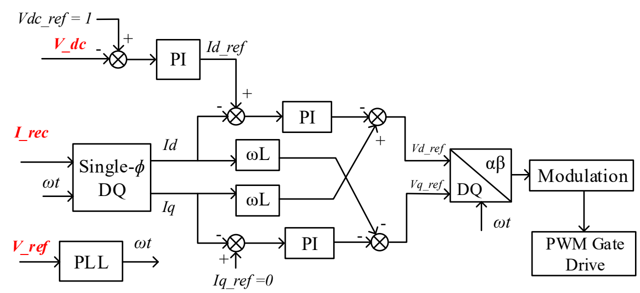

Figure 3.13 Rectifier control
(I_rec: rectifier input current, V_ref: source voltage, V_dc: DC bus voltage)

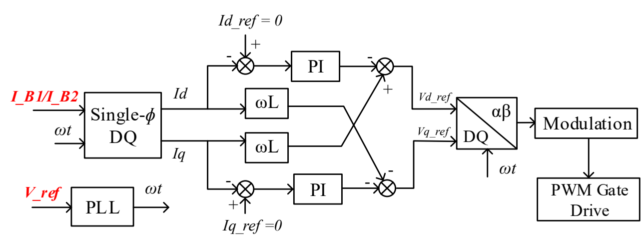

Figure 3.14 Inverter control
(I_B1/I_B2: upper/lower branch current, V_ref: source voltage)

3.4 Simulation Results

3.4.1 Series-connected Arcless SVR Simulation Results

A Matlab Simulink model is developed to resemble the proposed arcless tap changing operation for the medium voltage SVR. The simulation specifications are listed in Table I. It should be noted that the bias transformer secondary winding voltage of the

Table I SIMULATION SPECIFICATIONS

Source voltage	7620 V
Load current	1750 A
Tap voltage (V_{tap})	96 V
Equalizer winding voltage (V_{eq})	24 V
Bias winding voltage (V_{bias})	24 V
DC bus voltage	400 V
Converter capacity	42 kVA
System rated power	13.3 MVA
Converter switching frequency	10 kHz

lower branch is rated at 24 V while it takes the full load current during the upper branch current suppression. So, the inverter output power is only 0.3% of the system's full power rating. The operation sequence is the same as the process in Fig. 3.5. And Fig. 3.15 shows the arcless tap change without the improved compensation control method. Inverter starts

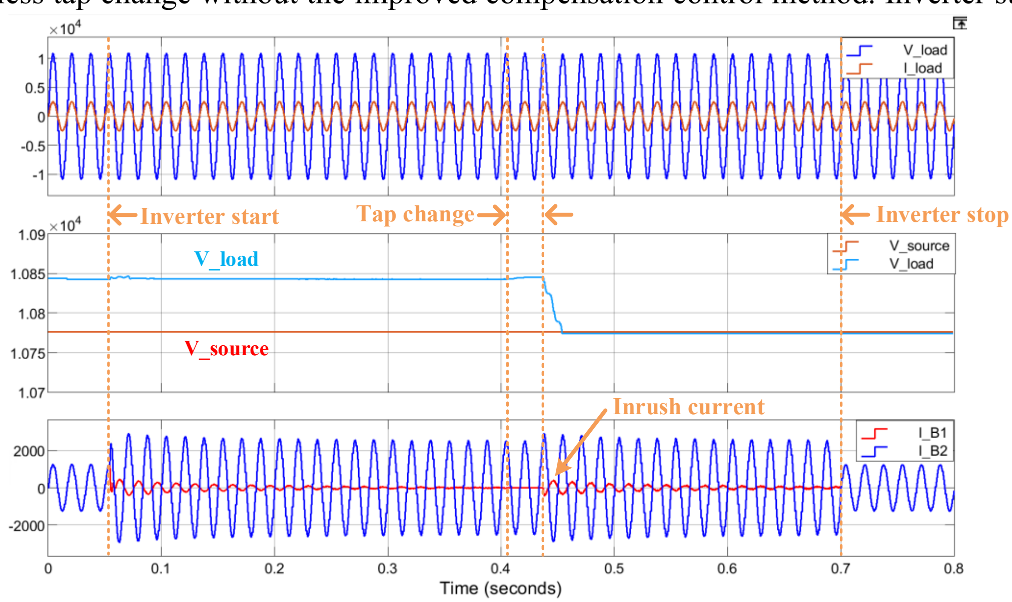

Figure 3.15 Arcless tap changing without compensation when PF = 1 (V_load: load voltage, *I_load*: load current, *V_source*: source voltage, *I_B1*: upper branch current, *I_B2*: lower branch current)

to work at 0.05 s and the upper branch current is suppressed to zero after a few cycles. Then, the mechanical tap change happens approximately from 0.41 s to 0.44 s. The source and load voltage peak values are displayed in the middle waveform. The load voltage change can be observed after the tap change. There is a measurement delay of the peak value since it calculates the sinusoidal wave magnitude for each cycle. A large inrush current can be observed in the upper branch as the contact makes to the next tap position at 0.44 s and the inverter requires a few cycles again to suppress *I_B1*. The inverter is disabled at 0.7 s. Due to the mechanical bouncing when the contact makes to the next tap position, the inrush current may cause an unnecessary bouncing arc on the contacts, which contributes to the acceleration of the metal contact erosion.

Fig. 3.16 is the arcless tap change waveform with the improved compensation control method. It can be noticed that there is no inrush current in the upper branch as the mechanical tap change completes at 0.44 s. The controller quickly adapts to the new tap position and the current is still regulated to zero. So, the inverter can be shut down earlier at 0.5 s and the arcless tap change process is completed.

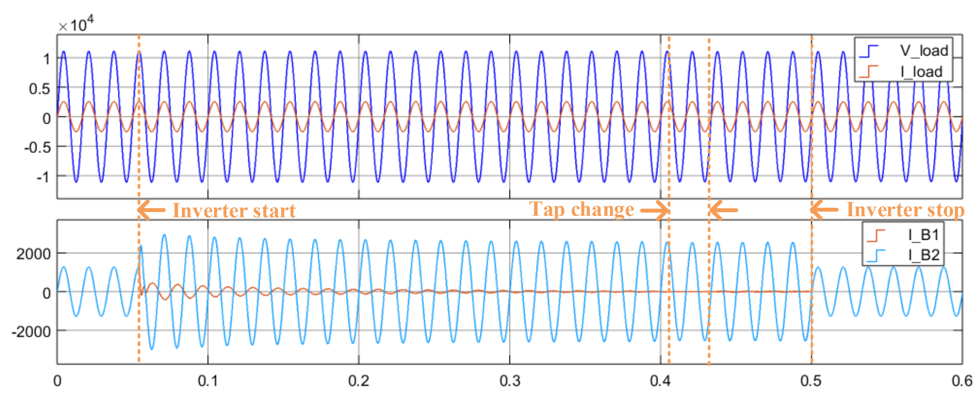

Figure 3.16 Arcless tap changing with compensation when PF = 1 (*V_load*: load voltage, *I_load*: load current, *I_B1*: upper branch current, *I_B2*: lower branch current)

Fig. 3.17 shows the comparison of the improved control method with the same *Vd* compensation value under the 0.8 load power factor. The results correspond with the previous model analysis that the load power factor does not affect the performance of the inverter control with the same *Vd* compensation value. The proposed controller compensation method works for current suppression under different power factors.

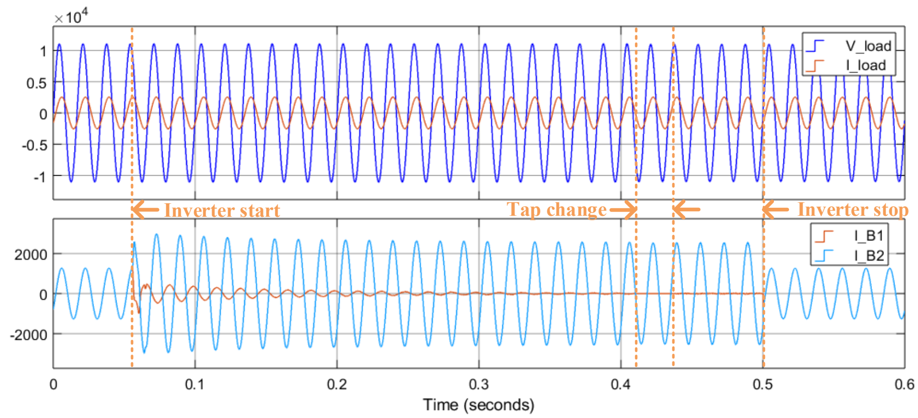

Figure 3.17 Arcless tap changing with compensation when PF = 0.8 (*V_load*: load voltage, *I_load*: load current, *I_B1*: upper branch current, *I_B2*: lower branch current)

3.4.2 Parallel Converter Based Arcless SVR Simulation Results

A simulation model of topology in Fig.3.4 is developed in Matlab Simulink. The simulation condition is listed in Table II. The emulated tap change operation sequence is exactly the same as the illustration in Fig. 3.6 that the upper branch moves from tap #1 to tap N. Based on equation (13) - (17), for the tap voltage V_{tap} of 96 V, the required inverter output voltage for current suppression is 48 V and the inverter current is half of the load current. The back-to-back converter power rating is 21 kW, while the total system power is 6.67 MW. By comparing the power capacity requirements of both the voltage regulator

Table II SIMULATION SPECIFICATIONS

Parameter	Value
Source voltage	7620 V
Tap voltage	96 V
DC bus voltage	400 V
Load current	875 A
Converter switching frequency	10 kHz

and the back-to-back converter, it is noticed that the required power capacity of the converter for current suppression is only 0.3% of the SVR total power capacity. Therefore, the proposed method only requires a fractional-rated power converter to achieve the arcless tap change operation.

According to the simulation results shown in Fig. 7, a complete arcless tap changing operation is conducted and the target branch current can be suppressed to zero. To be more specific for the timings, the inverter begins to work at T0. The target branch current *I_B1* can be suppressed to zero within a few cycles, which provides the condition for the arcless tap changing for the upper branch, while *I_B2* takes all of the load current. From T1 to T2, the upper branch moves mechanically from tap #1 to tap N. After T2, the two contacts are in the non-bridging position and are both on tap N. The controller adapts to the new tap status and the upper branch current is still suppressed to zero since the inverter is still on at the time. When the inverter is off at T3, upper branch *I_B1* and lower branch *I_B2* share

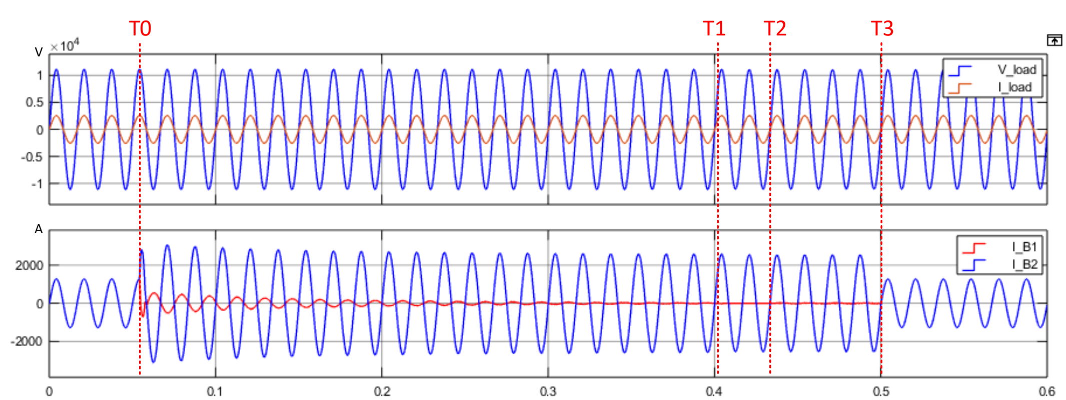

Figure 3.18 Proposed arcless step voltage regulator simulation results

the load current equally again. The arcless tap change operation is completed and the proposed arcless SVR simulation is verified.

3.5 Prototype Test Results

3.5.1 Series-connected Arcless SVR Prototype Test Results

To further evaluate the performance of the proposed arcless voltage regulator, Fig. 3.19 shows the scaled-down prototype that is developed in the lab. The prototype has 5 taps with ± 4 taps regulation range. The test specifications are listed in Table III. When it comes to the inverter capacity ratio compared to the system power in the prototype tests, the ratio is directly related with the ratio between the bias winding voltage and the source voltage. This is the reason that the advantage of fractionally rated converter rating is not reflected in the scaled-down prototype, but in the full-scale system simulation. An interface board is also designed and manufactured to communicate between the back-to-back converter, DSP controller and the tap changer controller.

Table III PROTOTYPE TEST SPECIFICATIONS

Source voltage	60 V
Load current	10 A
Tap voltage (V_{tap})	24 V
Equalizer winding voltage (V_{eq})	6 V
Bias winding voltage (V_{bias})	6 V
DC bus voltage	100 V
Converter capacity	60 VA
System power rating	600 VA
Converter switching frequency	10 kHz

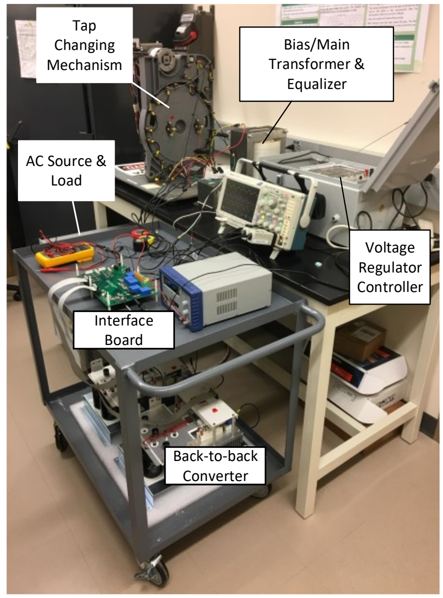

Figure 3.19 Proposed arcless step voltage regulator prototype

Tap lowering test is conducted with the same operation sequence in the simulation and the transient performance can be seen from the results in Fig. 3.20 and Fig. 3.21. The timing labels in the waveforms represent the same operations. The rectifier keeps working to regulate the DC bus voltage. Inverter starts to work at T0. The target branch current can be suppressed to zero after 6 cycles. When the upper branch current is suppressed to zero, the mechanical tap change begins from T1 to T2, where there is a 33 ms time window for the compensation signal implementation. The 33 ms is the time needed for the physical movement of the mechanical tap change, which may vary for different types of tap changers. The delay between the tap change trigger signal and the actual mechanical tap change is caused by the control and motor drive delay in the tap changer controller and the tap changing mechanism. Then, the inverter is shut down at T3. Inrush current is eliminated by the improved inverter control. The compensation signal is implemented between T1 and T2. The proposed Vd compensation method is verified by the hardware experiments. The Vd compensation can help to suppress the target branch current after the tap change and avoid the electric arc due to the mechanical bouncing when the tap makes to the next position.

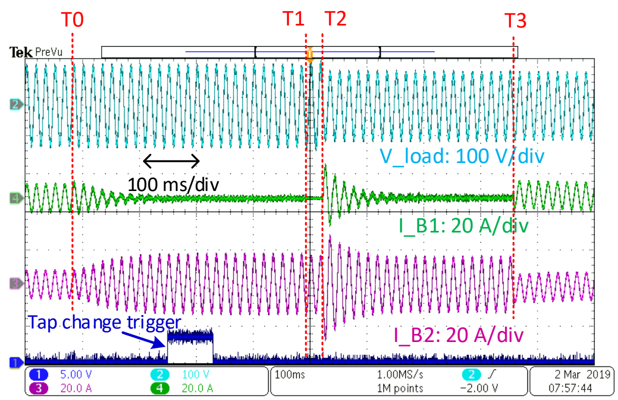

Figure 3.20 Tap change waveform without Vd compensation

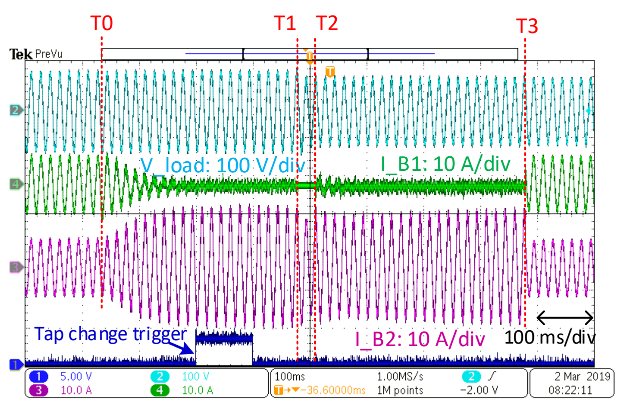

Figure 3.21 Tap change waveform with Vd compensation

The zoom-in waveforms are captured to investigate the arc details of the mechanical tap separation. A detailed arc comparison with the conventional voltage regulator when taps separate is also presented in Fig. 3.22. The contact voltage, *Vcontact*, refers to the voltage between the upper branch metal contact and the tap 1 contact. The criteria to determine the existence of the arc is when both the contact voltage and the upper branch current *I_B1* are non-zero. So, the arc in Fig. 3.22 (a) and the spark in Fig. 3.22 (b) are indicated in the dashed circle. In Fig. 3.22 (b), it can be noticed that there is the *I_B1* current re-conduction after it first goes to zero when contacts separate and a few electrical sparks still exist. The reason is that it takes a distance and a short time for two metal contact pads to completely separate, during which time there are mechanical friction and metal contact bouncing. Therefore, the sparks are caused by the contact mechanical bouncing and reconnection, which is unavoidable. According to [40], the electric contacts material erosion caused by electric arc can be quantified as erosion rate in equation (18), where k_I is the erosion coefficient that varies for different materials, for example, k_I is 2.4 for copper.

$$dG/dt = k_I I^{1.6} \ \mu g/s \tag{18}$$

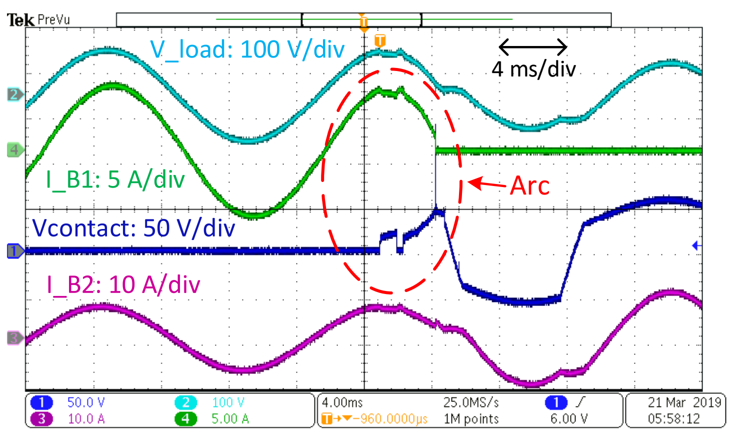

(a)

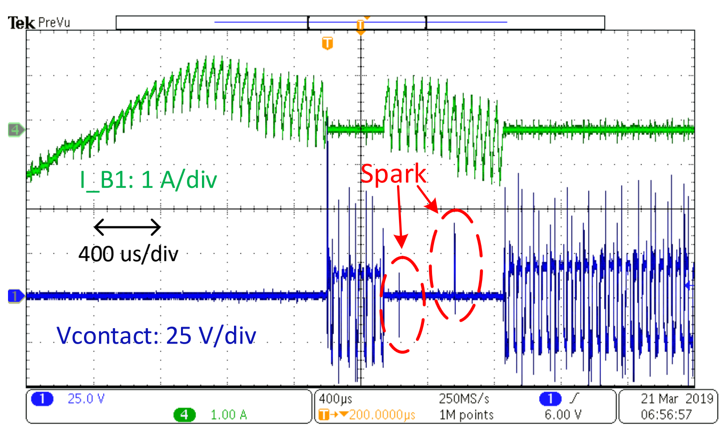

(b)

Figure 3.22 (a) Conventional SVR tap changing waveform, (b) Proposed arcless SVR tap changing waveform

Since coefficient k_I is related to the contact material, a comparison can be made based on the $I^{1.6}$ integration when *Vcontact* is not zero. By waveform import and calculation in Matlab, the ampere-second number of the $I^{1.6}$ integration is 4×10^{-6} as for arcless tap changing and 0.047 as for conventional tap changing which is 11,750 times of the arcless tap changing. The difference can be even larger in the full-scale medium voltage application since the load current is much higher. And the arc can be more difficult to extinguish for the conventional SVR in the full-scale model. So, the arc is significantly eliminated and the arcless tap changing is achieved successfully. The contact erosion rate of the proposed SVR is significantly reduced by more than 10,000 times when compared to the conventional SVRs.

Fig. 3.23 shows the zoom-in waveforms from T1 to T2 in Fig. 3.20 and Fig. 3.21. For the arcless tap change without compensation, the load voltage changes when the contact makes to the next tap position. And the load voltage change point is advanced when the Vd is compensated in the 33 ms mechanical tap change time window, which means the inverter output voltage already helps the load voltage to make the transition to the next status. Conventionally, the SVR switches tap very quickly. In the proposed arcless SVR operation, the load voltage change does not need to wait for the mechanical tap change to be completed. The compensation method makes it possible for advanced load voltage regulation with very high resolution and faster response while only one contact carries the load. On the other hand, the tap change mechanism in the proposed arcless SVR can move slower to relieve the mechanical stress while the voltage regulation can still be implemented with only one contact connected to the load during the tap change transient.

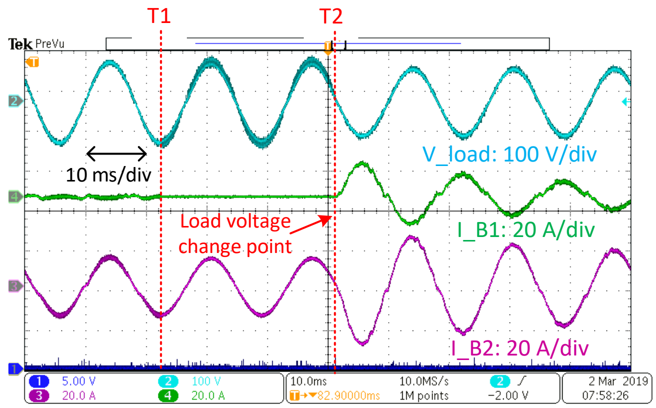

(a)

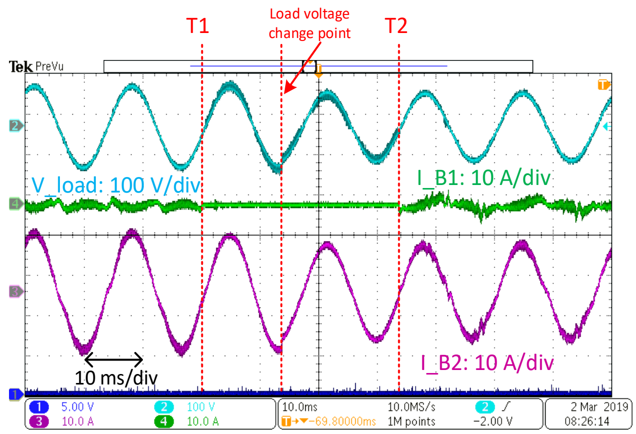

(b)

Figure 3.23 Load voltage change timing: (a) without compensation, (b) with compensation

Additionally, with a rectifier coupled in the main transformer, reactive power can be generated or absorbed from the rectifier by adjusting the *Iq_ref* in the rectifier control algorithm. Var control functionality is verified by the waveforms in Fig. 3.24. The load is an inductive load with power factor of 0.97. After implementing the proper rectifier current control, the rectifier generates reactive power and compensates the source power factor to 1.

The detailed model analysis and improved control method are presented to achieve better transient performance for tap position instant change. Simulation is firstly implemented to verify the control algorithms. A hardware prototype is developed for further evaluation. Based on the hardware test results, the proposed arcless voltage regulator can eliminate the arc by suppressing one target branch current before the mechanical tap changing movement. Arc comparison with the conventional SVR is also conducted based on the arc erosion rate. More practical functionalities, such as reactive power compensation and advanced load voltage regulation, are verified on the proposed arcless voltage regulator. This method is based on the conventional voltage regulator and introduces a partial-rated power converter to achieve the arcless tap change operation. The proposed method can extend the lifetime and the maintenance period of the SVR. Furthermore, the proposed arcless SVR integrates more functionalities, such as advanced load voltage regulation and volt/var control, in a single piece of equipment, so it shares the function of other similar devices, such as static synchronous compensators, in the existing

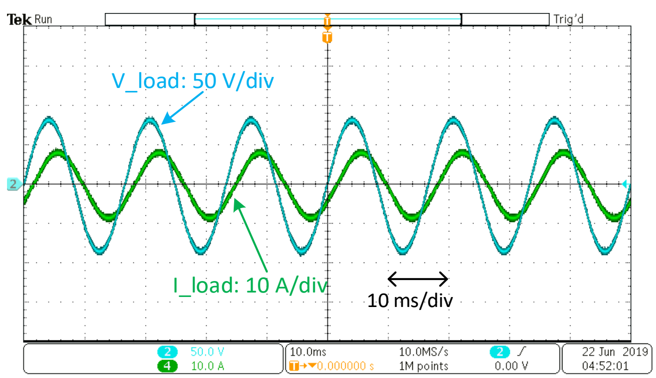

(a)

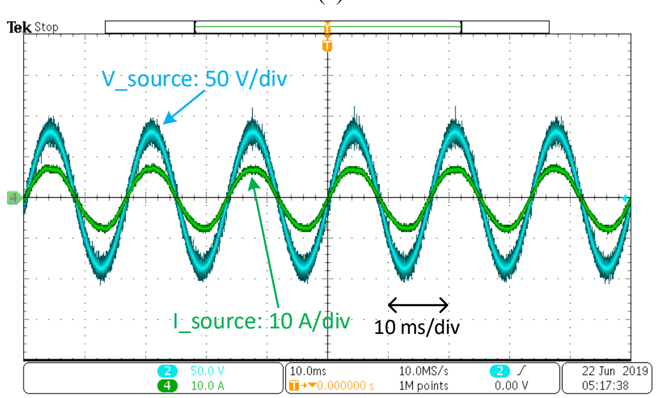

(b)

Figure 3.24 (a) Load waveforms PF = 0.97, (b) source waveforms PF = 1 distribution systems, which can eventually bring more flexibility to the planning and operation of the distribution system. The proposed topology requires minimum modification of the conventional SVR and is focused on the arc elimination to extend the lifetime of the SVRs, while most parts of the original tap changer configuration are kept unchanged. The simple upgrade makes it easier for the proposed arcless SVR to be widely implemented to the existing power distribution systems.

3.5.2 Parallel Converter Based Arcless SVR Prototype Test Results

To further evaluate the performance of the proposed arcless voltage regulator, a scaled-down prototype is implemented in the lab. Hardware prototype tests are also conducted. The test specifications are listed in Table IV.

Table IV PROTOTYPE TEST SPECIFICATIONS

Parameter	**Value**
Source voltage	60 V
DC bus voltage	100 V
Load current	10 A
Resistive load	6 Ω
Converter switching frequency	10 kHz

Tap lowering test is conducted and transient performance can be seen from the results in Fig. 3.25 and Fig. 3.26. In Fig. 3.25, the mechanical tap change happens at the dashed red line. After the mechanical tap change, both voltage and current of the load are lowered. The proposed arcless operation does not affect the conventional voltage regulation as the main function of the SVR. The power converter only affects the current distribution in the upper and lower branches by injecting an additional voltage in the branch loop. The operation sequence and the corresponding timing marks in Fig. 3.26 are the same as in the simulation. The inverter starts to work at T0 and the upper branch current is suppressed to zero after few cycles. The actual mechanical tap change happens from T1 to T2. Then, the upper branch current I_B1 can still be suppressed to zero after T2 to avoid the arcing due to the metal contacts bouncing. The upper branch current I_B1 can be suppressed to zero before and after the mechanical tap change. What remains in the steady-state waveform of the upper branch current I_B1 are just small current zero-crossings under the switching frequency, which is unavoidable due to the small leakage inductance in the tapped winding loop. Eventually, the inverter stops at T3 and the upper and lower branch share the load current equally again. Since the converter only operates during the arcless

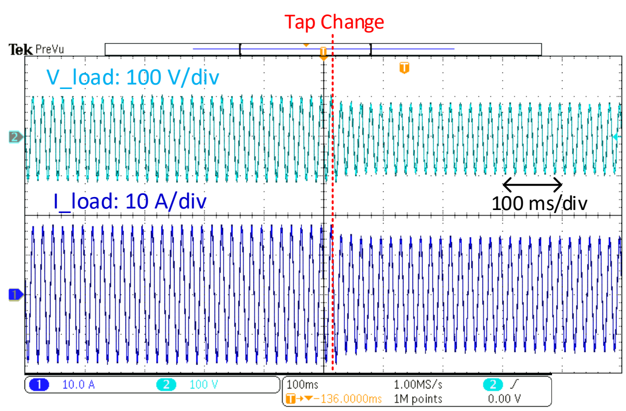

Figure 3.25 Load voltage and current waveform

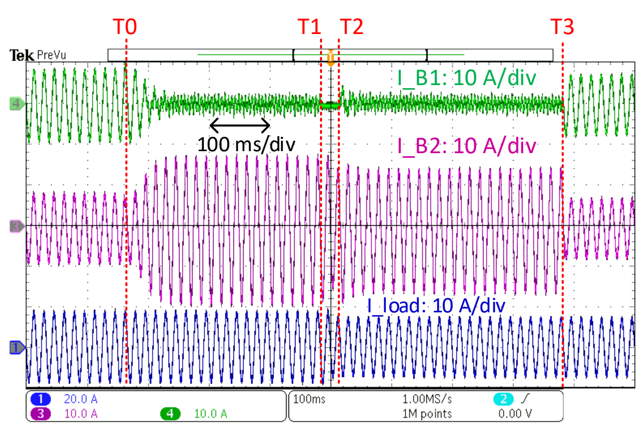

Figure 3.26 Branch and load current waveform

tap changing operation and the load current is conducted by the metal conductor paths during the normal operation, the proposed method does not influence the system efficiency.

Further investigation of the arc impact is conducted as the detailed arc waveforms are captured when the two energized contacts separate, which is shown in Fig. 3.27. Vcontact stands for the contact voltage between the upper branch metal contact and the tap #1 contact. The criteria to determine the existence of arc is that both the contact voltage and the upper branch current I_B1 are non-zero. It can be observed in Fig. 3.27 (b) that the electrical sparks still exist since the I_B1 current is re-conducted after it first goes to zero when contacts separate. This is because the two square-shaped metal contact pads require a distance and a short time to fully separate. The mechanical friction and metal contact bouncing may cause sparks and re-connection, which is unavoidable. The electric contacts

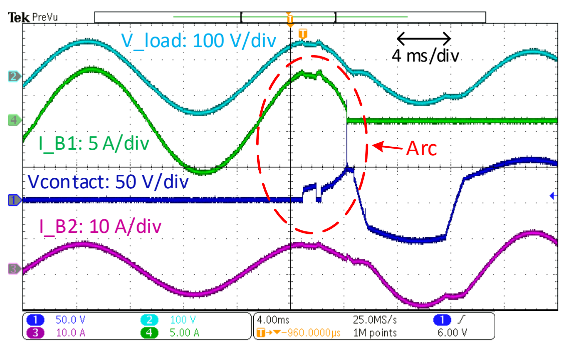

(a)

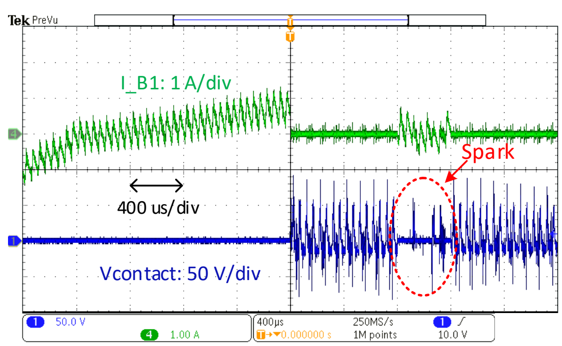

(b)

Figure 3.27 (a) Conventional SVR tap changing waveform, (b) Proposed arcless SVR tap changing waveform material erosion rate can be quantified by the equation provided in the previous subsection where k_I is the erosion coefficient that varies for different materials.

Comparison can be made based on the $I^{1.6}$ integration when Vcontact is not zero. By waveform data points import and calculation in Matlab, the ampere-second number of the $I^{1.6}$ integration is 4.2×10^{-6} As for the arcless SVR and 0.0465 As for the conventional SVR which is 11071 times of the arcless SVR. The difference can be even larger in the full-scale system as the load current is higher, where the arc can be more difficult to extinguish for the conventional SVR. Therefore, the contact erosion can be significantly eliminated with the proposed arcless tap change solution.

In this paralleled converter-assisted arcless SVR, simulation is firstly conducted to verify the control algorithms and concepts. A hardware prototype is developed for further evaluation. Based on the hardware testing results, the proposed arcless voltage regulator can eliminate the arc by suppressing one target branch current before the mechanical tap changing movement. By the arc impact analysis, the proposed method can significantly reduce the metal contact material erosion rate, hence extend the lifetime and maintenance period of the SVR. This method introduces a fractional-rated power converter to the system and the system total efficiency is not affected during the normal operation. More advanced functionalities, such as Var control and accurate voltage regulation, can be further developed for the proposed arcless step voltage regulator in the future.

CHAPTER 4: PROPOSED HYBRID VOLTAGE REGULATOR

4.1 Circuit Topology

The conventional SVR consists of the main transformer, preventive transformer, equalizer windings, and the tap change mechanism. The preventive transformer acts as a mutual inductance to suppress the circulating current in the branch loop. The upper and lower branch shares the load current equally. The equalizer windings are on the same magnetic core of the main transformer to balance the preventive transformer duty under the bridging and non-bridging positions. The proposed voltage regulator topology is shown in Fig. 4.1. Minimum modifications are made based on conventional SVR. The hybrid voltage regulator combines the conventional SVR with a fractionally rated power converter. Additional winding is added to the preventive transformer to become the bias transformer. The regulation transformer is connected in series with the load to compensate for the load voltage. The back-to-back converter, which consists of Converter 1 and Converter 2 in Fig. 4.1, can handle bidirectional power flow to support different functional requirements.

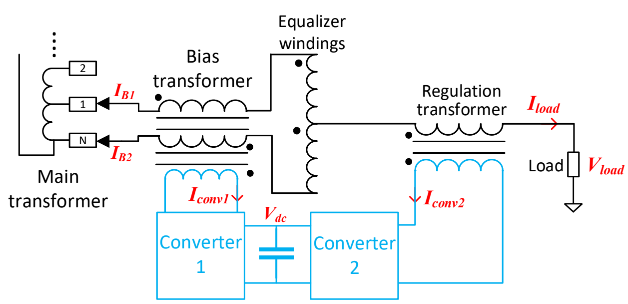

Figure 4.1 Proposed hybrid voltage regulator with back-to-back power converter

The principle of arcless tap change is that the target branch current needs to be suppressed to zero before mechanical tap change to avoid an electric arc. The equivalent circuits of the branch loop are illustrated in Fig. 4.2. Equalizer winding voltages are V_{eq1} and V_{eq2}. And bias winding voltages are V_{bias1} and V_{bias2}. V_{tap} represents the voltage between adjacent taps. The bias transformer also acts as a mutual inductor to suppress the circulating current in the branch loop. The leakage inductances of the upper and lower branch are L_{B1} and L_{B2}, respectively. L_{M21} and L_{M12} are the equivalent mutual inductance between the two windings of the bias transformer to suppress the circulating current. The circulating current is also necessary to balance the voltage difference in the branch loop. Converter 1 is connected to the third winding of the bias transformer and V_{conv1} is the input voltage of Converter 1. Converter 2 is connected to the regulation transformer and V_{conv2} is the output voltage of Converter 2. V_{reg} is the injected voltage for the load voltage regulation. The voltage before the regulation transformer is V'_{load}. V_{load} and I_{load} are the load voltage and current.

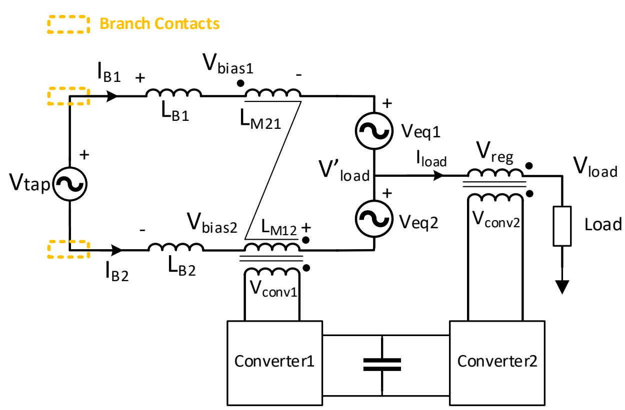

(a)

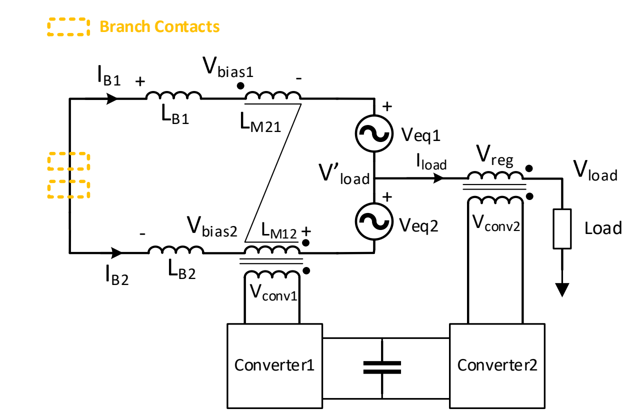

(b)

Figure 4.2 Equivalent circuits: (a) bridging position, (b)non-bridging position

When Converter 1 works to suppress the branch current to zero in the arcless tap change operation, the required output voltage polarities of the Converter 1 are opposite for the bridging and non-bridging positions. The power flow directions of Converter 1 are also opposite at the two positions. The current distribution difference between B1 and B2 determines the power flowing through Converter 1. The compensation for voltage sag and swell also requires Converter 2 to have two opposite power flow directions. Under the voltage regulation mode, Converter 1 works as the rectifier and Converter 2 operates as the inverter to compensate for the load voltage. Under the arcless tap change mode, Converter 2 works as the rectifier, instead, to support Converter 1, which serves as the inverter, to suppress the branch current. For this reason, Converter 1 and Converter 2 can provide power for each other under different operation modes. Both arcless tap change operation and stepless voltage regulation can be achieved with a fractionally rated back-to-back power converter. Converter 1 and Converter 2 are designed to only compensate half of the step voltage, which is 0.31% of the SVR's output voltage. Therefore, the converter power ratings can be minimized to reduce the cost and efficiency impact on the traditional SVR system.

4.2 Principle of Arcless Tap Change Operation

To achieve the arcless tap change, the current in the target branch needs to be suppressed to zero before the mechanical tap change. Therefore, the arc can be eliminated when the metal contacts separate and the contact erosion rate can be significantly reduced. Fig. 4.3 illustrates a tap change sequence where the upper branch contact moves from tap 1 to tap N. The specific operations in Fig. 4.3 (a) – (d) are described below.Converter 1 is disabled and there is no current flowing at the input. Converter 2 works actively with current flowing through the regulation transformer to hold the DC bus voltage and avoid regulation transformer from core saturation.

(a) Converter 1 is disabled and there is no current flowing at the input. Converter 2 works actively with current flowing through the regulation transformer to hold the DC bus voltage and avoid regulation transformer from core saturation.

(b) Converter 1 starts to work and suppress the upper branch current IB1 to zero. The arrow between the two converters indicates the power flow direction.

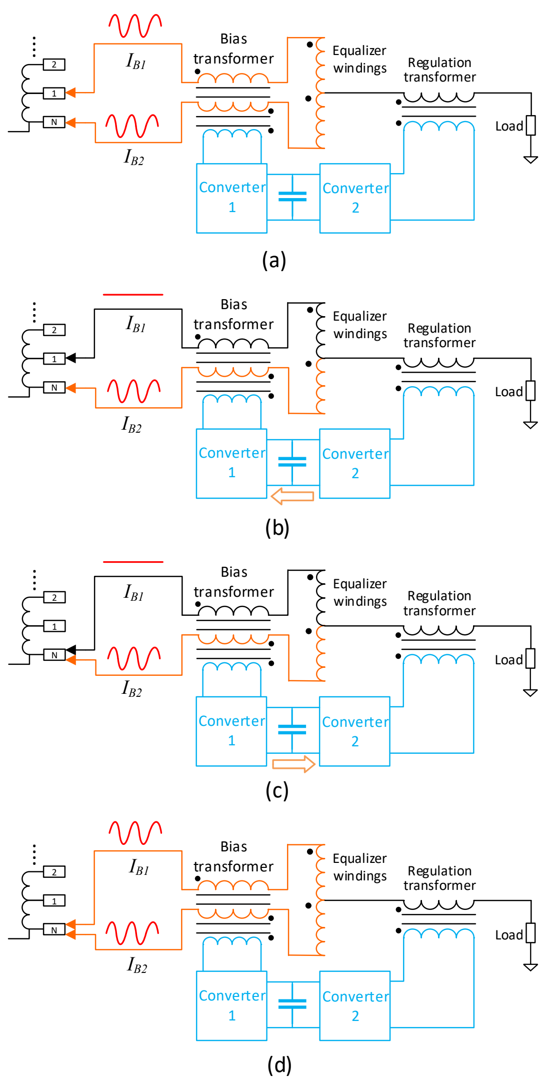

Figure 4.3 Arcless tap change operation sequence: (a) Converter 1 is disabled and Converter 2 regulates the DC bus voltage, (b) Upper branch current suppression, (c) Upper branch contact moves from tap 1 to tap N, (d) Converter 1 is shut down.

(c) Upper branch contact moves from tap 1 to tap N without arc while Converter 1 keeps working to ensure there is no current flowing through the upper branch. The power flow direction of the power converter is reversed, so the output voltage on the regulation transformer is also reversed.

(d) Converter 1 is shut down and the two branches share the load current again.

4.3 Principle of Stepless Voltage Regulation

In the proposed solution, the mechanical tap changer still makes tap changes to regulate large voltage steps, and the power converter injects a compensation voltage to regulate small voltage deviation between taps. As indicated in Fig. 4.3 (b) and (c), the power flow direction is reversed from the bridging to the non-bridging position. The current distribution difference between the upper and lower branches also requires different values of the power supplied from Converter 1. For the same reason, the power supplied to or absorbed from Converter 1 can also be utilized for Converter 2 to output different voltage to the regulation transformer. Based on the transformer turns ratio design, as shown in Fig. 4.4, there is certainly a regulation voltage range from Converter 2, but the output voltage from the regulation transformer can bridge the gap between each step voltage change. Fig. 4.5 (a) illustrates the conventional SVR load voltage relationship with the tap position where the load voltage is changed step by step for fixed source voltage. In the

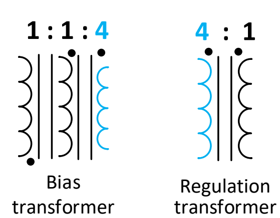

Figure 4.4 Transformer turns ratio

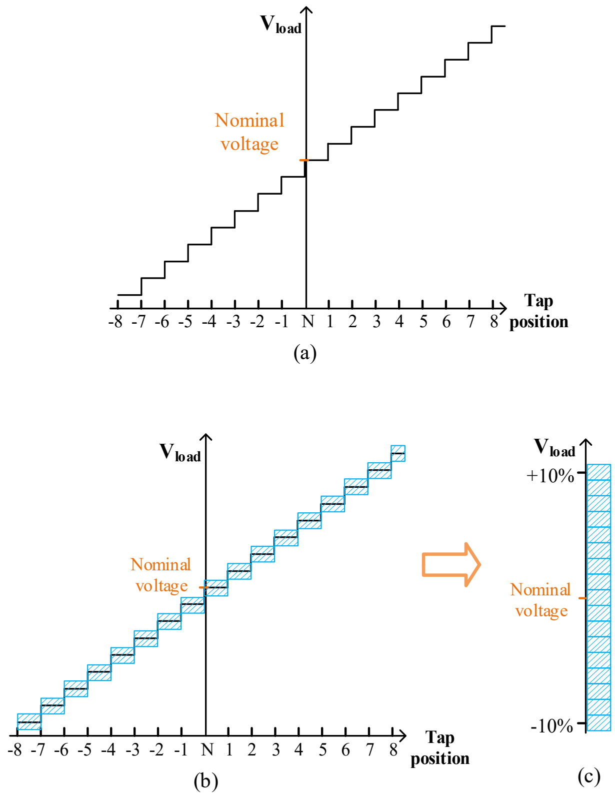

Figure 4.5 Load voltage regulation principle for fixed source voltage V_s: (a) The conventional SVR with step voltage change, (b) The proposed hybrid voltage regulator with positive and negative half step voltage regulation range for each tap position, (c) The full range of the proposed stepless voltage regulation

proposed hybrid voltage regulator, the voltage regulation range for each tap position is from negative to positive half-step voltage as the blue-shaded area in Fig. 4.5 (b). The regulation ranges for each tap position eventually combine into a continuous and stepless load voltage regulation range of ±10%, as shown in Fig. 4.5 (c).

4.4 Circuit Analysis and Control

All the parameter and variable definitions are described in Section II and labeled in Fig. 5. Based on the system design and transformer turns ratio in Fig. 7, the winding voltages of the bias transformer are expressed by equation (19). The equalizer winding voltages are designed to be a quarter of the tap voltage as equation (20). For each tap change operation, only one tap contact moves to the other tap and two tap contacts are either at the bridging position or the non-bridging position. Therefore, the step voltage change V_{step} is half of the tap voltage V_{tap} as equation (21). Due to the existence of the circulating current in the branch loop, the upper and lower branches do not share exactly half of the load current. So, the upper branch current I_{B1} and lower branch current I_{B2} are derived as equations (22) and (23), respectively. The load current is the sum of I_{B1} and I_{B2}, as shown in equation (24). The injected voltage from the regulation transformer, V_{reg}, regulates the load voltage to the nominal value as equation (25).

$$V_{bias1} = V_{bias2} = \frac{1}{4} V_{conv1} \tag{19}$$

$$V_{eq1} = V_{eq2} = \frac{1}{4} V_{tap} \tag{20}$$

$$V_{step} = \frac{1}{2} V_{tap} \tag{21}$$

$$I_{B1} = \frac{1}{2} I_{load} + I_{circulating} \tag{22}$$

$$I_{B2} = \frac{1}{2} I_{load} - I_{circulating} \tag{23}$$

$$I_{load} = I_{B1} + I_{B2} \tag{24}$$

$$V_{load} = V'_{load} + V_{reg} \tag{25}$$

When two tap contacts are at the bridging position, the voltage sum of bias windings and equalizer windings is equal to the tap voltage as equation (26). By solving equations (19), (20), and (26), bias winding voltages are derived as equation (27). The circulating current can be expressed as equation (28).

$$V_{tap} = V_{bias1} + V_{bias2} + V_{eq1} + V_{eq2} \tag{26}$$

$$V_{bias1} = V_{bias2} = \frac{1}{4} V_{tap} \tag{27}$$

$$I_{cirulating} = \frac{1}{2} V_{tap} / \omega (L_{B1} + L_{B2} + L_{M21} + L_{M12}) \tag{28}$$

When two tap contacts are at the non-bridging position, the bias winding voltages are equal to the equalizer winding voltages in a reverse polarity as equation (29). By solving equations (19), (20), and (29), bias winding voltages are derived as equation (30). The circulating current can be expressed as equation (31) and it is in the reverse polarity of which in the bridging position.

$$V_{eq1} + V_{eq2} = -(V_{bias1} + V_{bias2}) \tag{29}$$

$$V_{bias1} = V_{bias2} = -\frac{1}{4}V_{tap} \tag{30}$$

$$I_{cirulating} = -\frac{1}{2}V_{tap}/\omega(L_{B1} + L_{B2} + L_{M21} + L_{M12}) \tag{31}$$

For the arcless tap change operation, Converter 1 does not change the voltage distribution in the branch loop but regulates the target branch current to zero by injecting current through the connected winding of the bias transformer under current control mode.

For the load voltage regulation, the maximum and minimum voltage injections to the load are analyzed by the power balance law between two power converters. When the load power factor is unity, only the active power delivered between two converters is used for the load voltage regulation, which also applies to most SVRs in the distribution system. Since all winding voltages in the branch loop are in phase with the source and load voltages, the circulating current only affects the reactive power and it can be neglected for converter active power analysis.

When all the load current flows through the upper branch, the active power absorbed by Converter 1 is expressed as equation (32). The voltage and current relationships of the regulation transformer windings are expressed by equations (33) and (34) based on the turns ratio. Hence, the active power of Converter 2 is expressed as equation (35). Because of the power balance between two converters as equation (36), the maximum injected regulation voltage is derived as equation (37) by solving equations (32), (35), and (36).

$$P_{conv1} = V_{bias1} I_{B1} = V_{bias1} I_{load} = \frac{1}{4} V_{tap} I_{load} \tag{32}$$

$$V_{conv2} = 4V_{reg} \tag{33}$$

$$I_{conv2} = \frac{1}{4} I_{load} \tag{34}$$

$$P_{conv2} = V_{conv2} I_{conv2} = V_{reg} I_{load} \tag{35}$$

$$P_{conv1} = P_{conv2} \tag{36}$$

$$V_{reg\_max} = \frac{1}{4} V_{tap} = \frac{1}{2} V_{step} \tag{37}$$

When all the load current flows through the lower branch, the active power generated by Converter 1 is expressed as equation (38). By solving equations (35), (36), and (38), the minimum injected regulation voltage is derived as equation (39).

$$P_{conv1} = -V_{bias2} I_{B2} = -V_{bias2} I_{load} = -\frac{1}{4} V_{tap} I_{load} \tag{38}$$

$$V_{reg\_min} = -\frac{1}{4} V_{tap} = -\frac{1}{2} V_{step} \tag{39}$$

Two different control strategies are implemented for two converters under the arcless mode and the regulation mode. Fig. 4.6 and Fig. 4.7 show control algorithms for two converters under the arcless mode and regulation mode, respectively. Parameter names in the control diagrams are marked in red in Fig. 4.1 correspondingly. V_s is the source voltage. V_{dc} is the DC bus voltage. I_{conv1} and I_{conv2} are the input current of Converter 1 and Converter 2. I_{B1} and I_{B2} are the upper and lower branch currents. V_{load} is the load voltage. Under the arcless mode in Fig. 4.6, Converter 2 works as the rectifier to regulate the DC bus voltage while Converter 1 works as the inverter to suppress the target branch current.

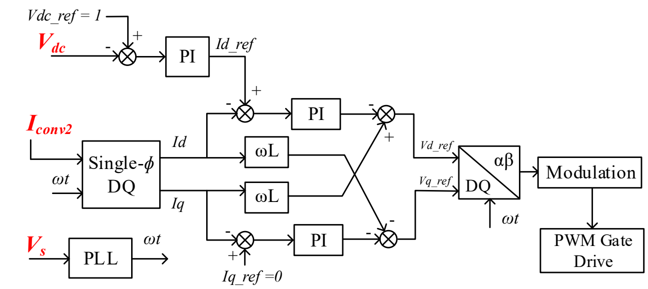

(a)

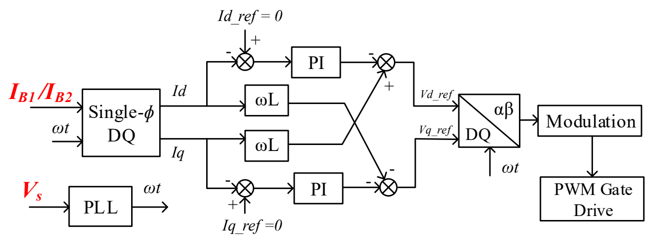

(b)

Figure 4.6 Arcless mode: (a) Converter 2 control, (b) Converter 1 control

Fig. 4.7 shows control algorithms for stepless load voltage regulation. Under the regulation mode, Converter 1 works as the rectifier to regulate the DC bus voltage while Converter 2 works as the inverter to compensate the load voltage to the nominal value. Different power draw from the bias transformer leads to different branch current distribution for I_{B1} and I_{B2}.

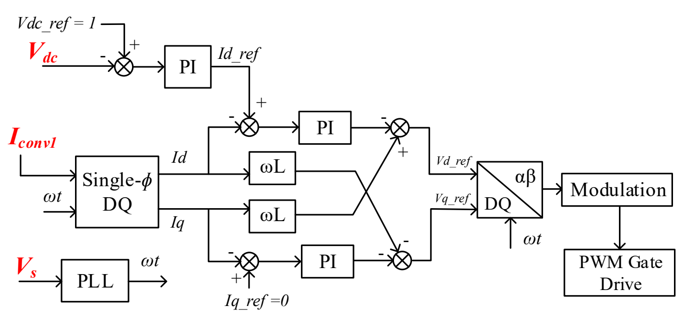

(a)

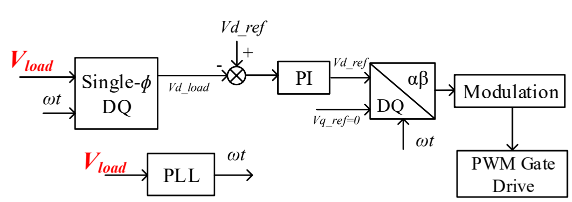

(b)

Figure 4.7 Regulation mode: (a) Converter 1 control, (b) Converter 2 control

4.5 Simulation Results

The full-scale simulation model of the device is developed in Matlab Simulink. The simulation parameters are listed in Table V. For the standard SVR ratings, the distribution transformer power rating is 2.6 MVA and the voltage regulation range is ±10% with ±8 taps in total. Every step voltage change is 48V which is half of the tap voltage. The proposed hybrid voltage regulator only requires 8.16 kVA converter capacity to cover the gap between each step voltage, which is 0.31% of the distribution transformer rating in the proposed hybrid voltage regulator.

Table V SIMULATION SPECIFICATIONS

Parameter	**Value**
Source voltage	7620 V
Load current	340 A
Tap voltage (V_{tap})	96 V
Equalizer winding voltage (V_{eq})	24 V
Bias winding voltage (V_{bias})	24 V
Regulation voltage range	±24V
DC bus voltage	400 V
Converter capacity	8.16 kVA
System rated power	2.6 MVA
Converter switching frequency	10 kHz

Fig. 4.8 shows the simulation results of a successful arcless tap change operation replicating the operation sequence shown in Fig. 4.3. The inverter, which is Converter 1 in the arcless tap change operation, starts to work at 0.1 s. The upper branch current I_{B1} is suppressed to zero before and after the mechanical tap change which happens at 0.5 s and ends at 0.54 s. The tap starts to move at 0.5 s when the upper branch current is suppressed to zero so that the arc can be eliminated for the mechanical tap change, which shows the

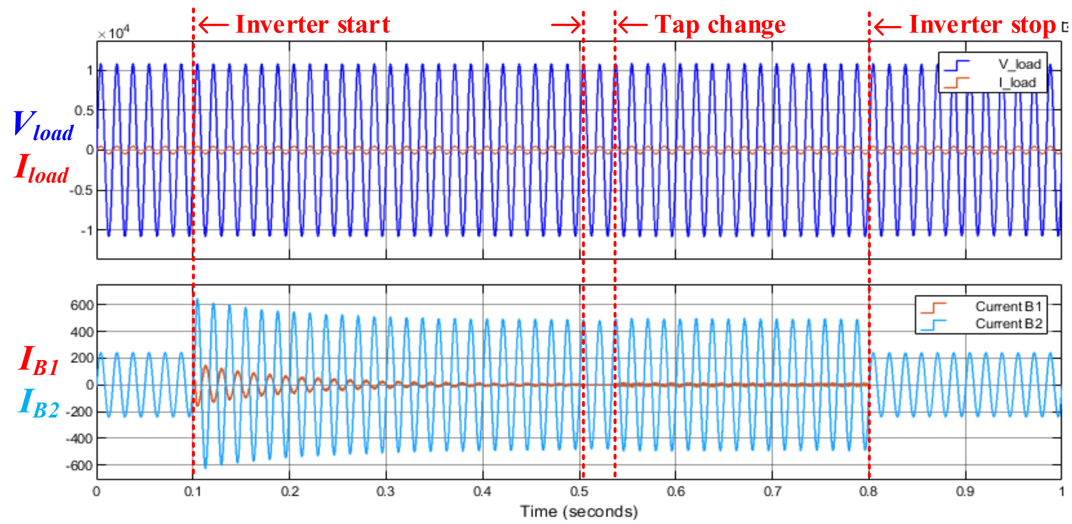

Figure 4.8 Arcless tap change mode simulation results

successful arcless tap change operation. The upper branch current I_{B1} keeps being suppressed to zero after the mechanical tap change to avoid possible tap contact bouncing arc. When the upper branch current is zero, the lower branch current I_{B2} is doubled when the load current flows entirely through the lower branch. Converter 1 is disabled at 0.8 s. Converter 2 proceeds to the next regulation range after the tap change.

System performance under the voltage regulation mode is presented in Fig. 4.9. To verify the stepless voltage regulation function, open-loop control is implemented for Converter 2. The output voltage of Converter 2 through the regulation transformer ramps up from -24 V to +24 V from 0.5 s to 2.7 s. Converter 1 works as the rectifier to provide power for Converter 2 under the regulation mode. During the voltage ramping-up, the load voltage can be regulated continuously from negative to positive half step voltage. Therefore, the stepless voltage regulation is achieved by the power converter injecting regulation voltage in series with the load. At 1.7 s, the load voltage reaches the nominal voltage of 7668 V at the bridging position. Load voltage increases as I_{B1} and I_{B2} have different distributions in the branches, which indicates the power flow change from the bias transformer. The load voltage

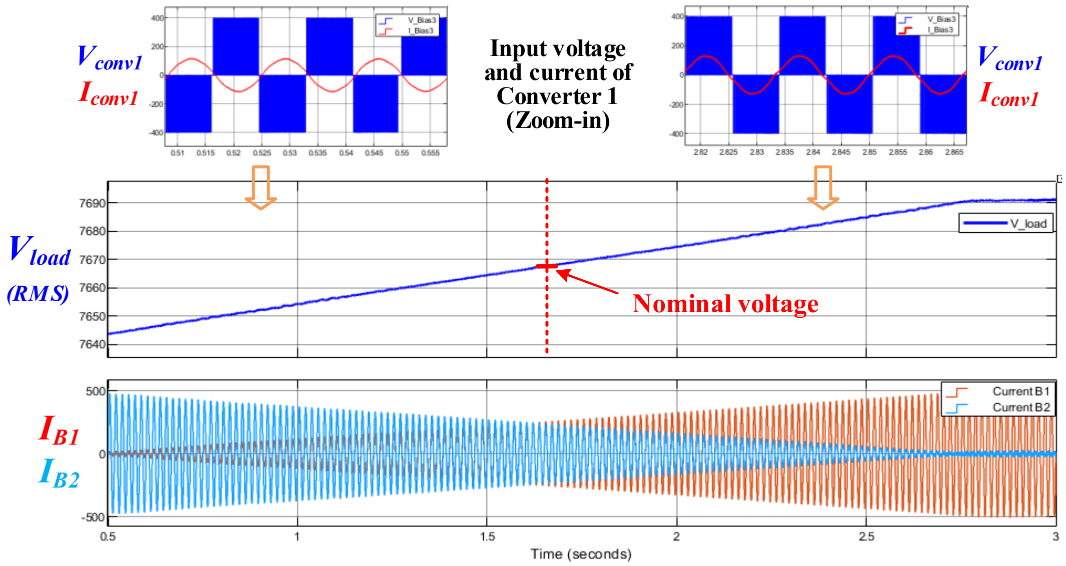

Figure 4.9 Voltage regulation mode simulation results

is below the nominal tap voltage before 1.7 s while Converter 1 absorbs active power from Converter 2, during which time I_{B2} is larger than I_{B1}. After 1.7 s, the load voltage is higher than the nominal tap voltage while Converter 1 generates active power from the bias transformer and supplies it to Converter 2, during which time I_{B1} becomes larger than I_{B2}. It is verified that different current distribution in the upper and lower branches can provide power for the load voltage regulation. In short, the two converters can support each other to achieve both arcless tap change and stepless load voltage regulation.

4.6 Converter Power Loss and System Efficiency

Since the power converter in the proposed hybrid voltage regulator works continuously to regulate the load voltage, the system efficiency impact needs to be evaluated. Based on the simulation specifications in Table V and the transformer turns ratio design, the 600V, 120A IGBT is selected as the device reference model [41]. The PLECS model of the selected IGBT is imported in PLECS for converter power loss simulation. PLECS simulation uses similar mathematical modeling for electric circuits as Matlab Simulink and it is also capable of device thermal simulation. The imported device PLECS model reflects the device switching and conduction losses simultaneously during the simulation by matching the device loss value accordingly with the instant device voltage, current, and temperature in a lookup table The simulation conditions are the same as the parameters in Table V. The steady-state IGBT case temperature is at 70 °C. The converter power loss is simulated for -24V, -12V, 0V, 12V, and 24V load voltage regulation, respectively. Different load voltage regulations correspond to different converter power and power flow direction.

Based on the PLECS simulation results, the converter power loss breakdown is shown in Fig 4.10. For the load voltage regulation mode, Converter 1 is the rectifier while Converter

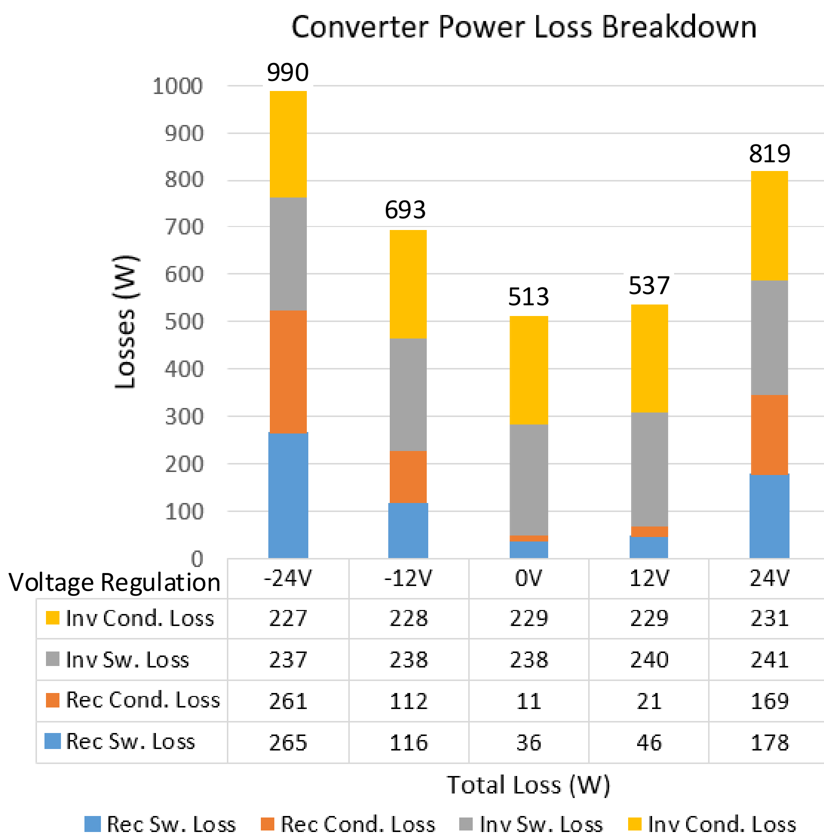

Figure 4.10 Converter power loss breakdown

2 serves as the inverter. Since the regulation transformer secondary side is coupled with the inverter (Converter 2) load current, the inverter conduction loss and switching loss do not change much when the load voltage regulation varies. However, the bias winding is a voltage source for Converter 1. The conduction loss and switching loss of the rectifier (Converter 1) change significantly when the load voltage regulation varies. The reason is that the Converter 1 input current from the bias winding changes along with the load voltage regulation.

The simulated total system efficiency is presented in Fig 4.11. The estimation assumes that the conventional SVR efficiency is 98%. Although the total converter power loss is up to 1 kW, the maximum converter power loss is less than 0.04% of the total system power. Therefore, the system efficiency impact from the power converter power loss can be negligible in the load voltage regulation. While the converter is at light load condition with poor converter efficiency at zero load voltage regulation, the absolute power loss is at the

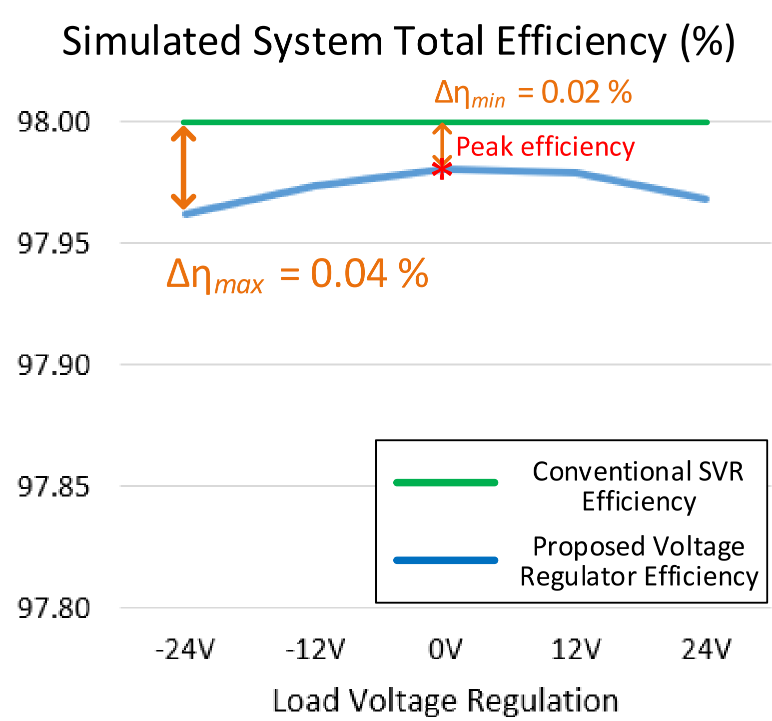

Figure 4.11 Simulated system total efficiency

minimum value for the system. So, the system peak efficiency of 97.98% happens at zero load voltage regulation condition, where the efficiency impact is only 0.02%.

4.7 Prototype Test Results

A scaled-down experimental platform is developed in the lab to evaluate the prototype performance, as shown in Fig. 4.12. The main transformer is a tap changer transformer with 5 taps. A tap changer mechanism and an Eaton CL-7 voltage regulator controller are utilized to make tap changes in the experiment. The source voltage is 240V and the load is rated at 288V, 10A, and 3 kW. The power converter DC bus voltage is designed as 200 V as the maximum injected voltage at the inverter side is 96 V. Other detailed parameters of the scaled-down prototype test are listed in Table. VI. It is noted that only the current rating and SVR's primary-side input voltage are scaled down in the experimental platform while the tap voltage and other winding voltages are the same with the medium-voltage model including the

Table VI PROTOTYPE TEST SPECIFICATIONS

Parameter	Value
Source voltage	240 V
Load voltage	288 V
Load current	10.5 A
Load power	3 kW
Tap voltage (Vtap)	96 V
Equalizer winding voltage (Veq)	24 V
Bias winding voltage (Vbias)	24 V
Regulation voltage range	±24 V
Maximum required converter power/percentage of the system	250W/8.4%
DC bus voltage	200 V
Converter switching frequency	10 kHz

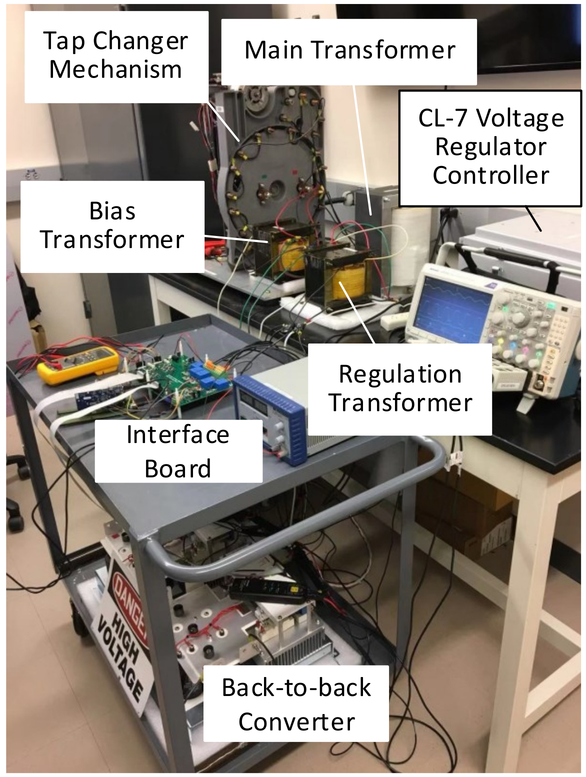

Figure 4.12 Proposed hybrid voltage regulator prototype

regulation voltage range. Therefore, the converter power percentage is 8.4% in the scale-down prototype. A DSP TI 28379D controller is used to implement the proposed arcless tap change and voltage regulation control. An interface board is designed to communicate between the DSP controller and the power converter.

Arcless tap change function is validated first when Converter 2 operates as the rectifier to regulate the DC bus voltage and provides power for Converter 1. The hardware tests show the full operation process of arcless tap change in Fig. 4.13 (a). When Converter 1 is started, the upper branch current I_{B1} is suppressed to zero after a few cycles and the lower branch current I_{B2} is doubled as the full load current is flowing through the lower branch. It can be observed that the upper branch current keeps being suppressed to zero before and after the tap change, which is contributed by the inverter output voltage compensation strategy proposed previously in the Section of Arcless Tap Change. As

Converter 1 is disabled after the tap change, the upper and lower branch share the load current equally again and the load voltage lowers down to the next step range. The load voltage and current waveforms during the arcless tap change are shown in Fig. 4.13 (b). After the mechanical tap change, the load voltage and current are lowered down. The upper and lower branch current distribution variation and the current rebalancing process do not affect the load voltage V_{load} and load current I_{load} sinusoidal waveforms.

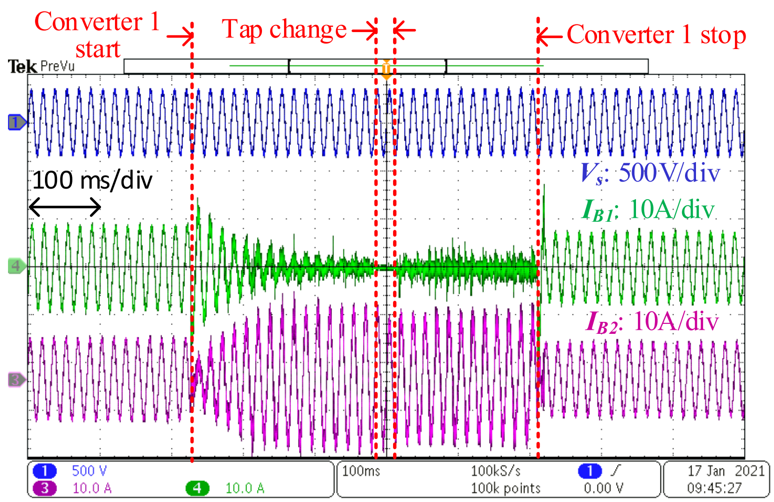

(a)

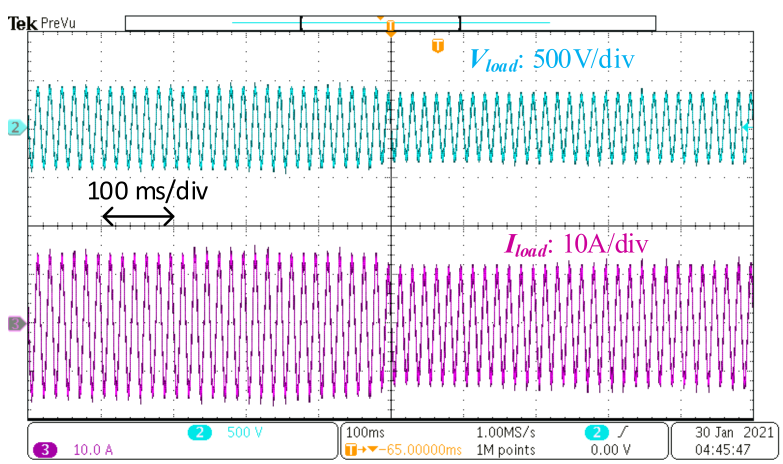

(b)

Figure 4.13 Arcless tap change waveforms: (a) full operation process, (b) load voltage and current waveform during the arcless tap change

To further evaluate the advantage of arcless tap change operation, the detailed electric arc impact comparison is shown in Fig. 4.14. The contact voltage $V_{contact}$ represents the voltage between the upper branch metal contact and the transformer tap contact. When tap contacts are separated from each other, $V_{contact}$ changes from zero to a non-zero value. Therefore, the criteria to determine the existence of the electric arc is when both the contact voltage and the upper branch current I_{B1} are non-zero. And the electric arc in Fig. 4.14 (a) and the sparks in Fig. 4.14 (b) are indicated accordingly. In Fig. 4.14 (b), I_{B1} is re-conducted after it first goes to zero and a few sparks also exist. The reason is that it takes a distance and a short time for two metal contacts to completely separate. And it is unavoidable to

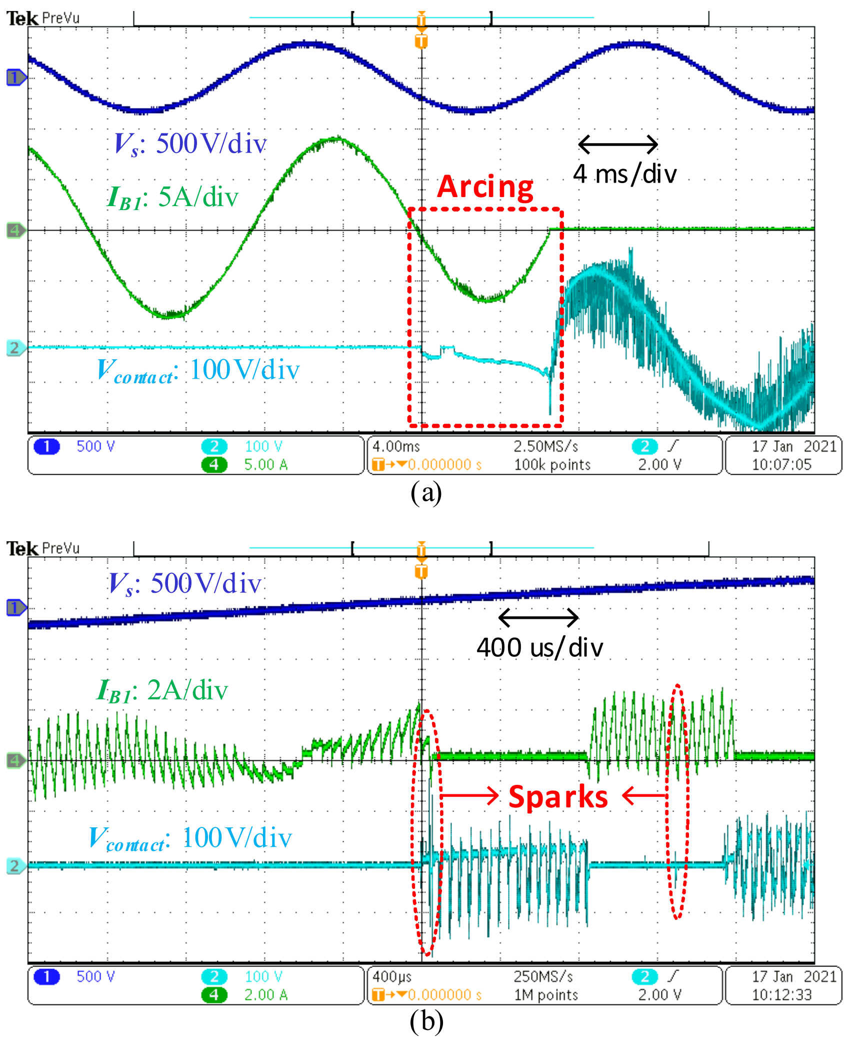

Figure 4.14 (a) Conventional SVR tap change waveform, (b) Arcless tap change waveform

have the contact mechanical bouncing and reconnection during the mechanical tap separating movement.

The current data are collected from the oscilloscope and processed in Matlab. And the ampere-second number of the $I^{1.6}$ integration, in Equation (18), is 0.077 As for the conventional tap change with arc and 7.3×10^{-5} As for the arcless tap change. Based on the scale-down experiments, the contact erosion rate of the arcless tap change is significantly reduced by 1055 times compared with the conventional mechanical tap change with the arc. The erosion rate difference can be even more significant in the medium voltage SVR since the load current is much higher than the scale-down prototype and it is more difficult to extinguish the electric arc.

Therefore, the electric arc of the mechanical tap change is eliminated and the proposed arcless tap change operation is achieved successfully.

For the voltage regulation function, Fig. 4.15 (a) illustrates the load voltage is regulated to 288 V while the source voltage ramps up from 220 V to 260 V. The equivalent load voltage variation is ±24 V. Close-loop control is achieved in the load voltage regulation hardware test. As the source voltage changes below and beyond the nominal value of 240 V, the injected regulation voltage changes from +24 V to -24 V. It determines the power flow direction between the power converters, which eventually influences the current distribution in the upper and lower branches. Therefore, different I_{B1} and I_{B2} distribution can be observed as the source voltage changes. As indicated by the dashed line in Fig. 4.15 (a), the source voltage increases from 220 V to 260 V maximum value. When the source voltage is below 240 V, the upper branch current I_{B1} is larger than the lower branch current I_{B2} and Converter 1 provides active power for Converter 2 to increase the load voltage to the nominal value of 288 V. When the source voltage is beyond 240 V, the upper branch current I_{B1} becomes smaller than the lower branch current I_{B2} and Converter 1 absorbs active power

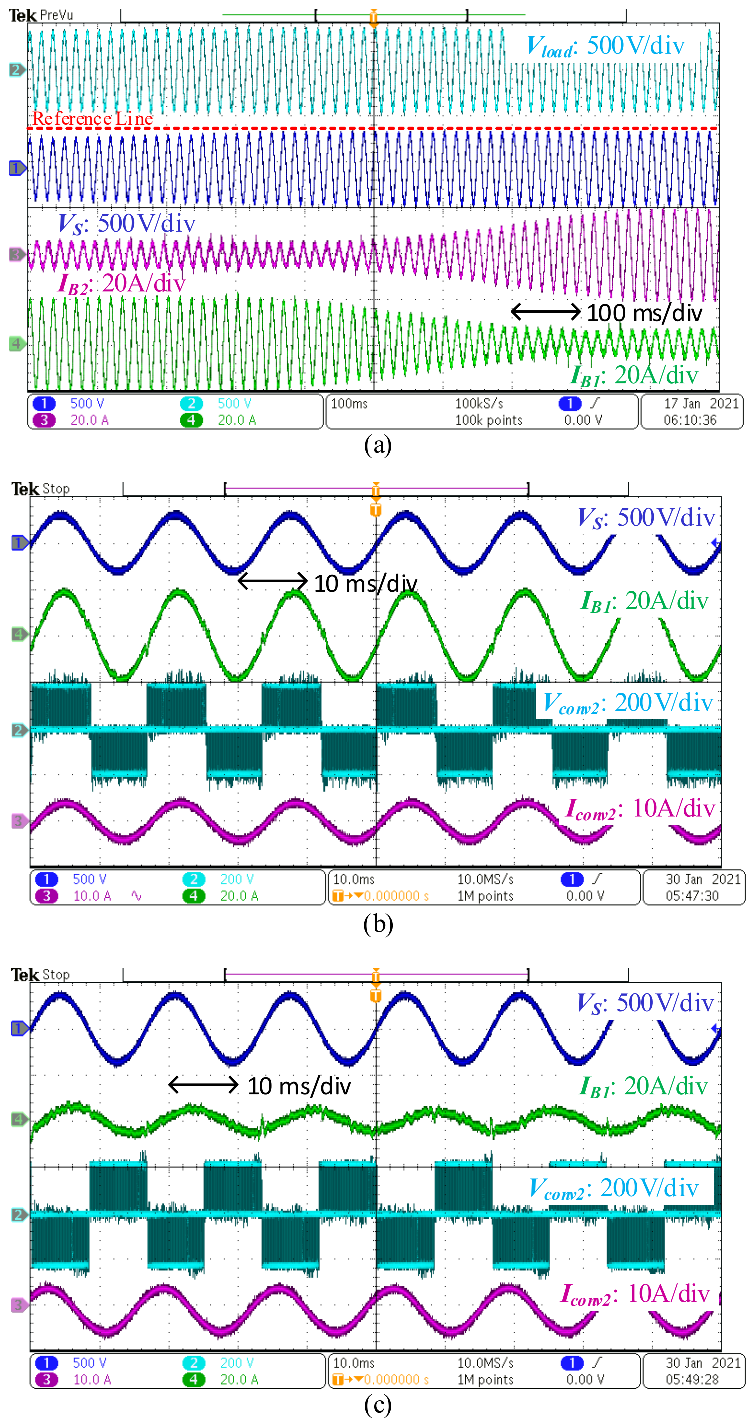

Figure 4.15 Voltage regulation waveforms: (a) branch currents and voltage waveforms of the source and load, (b) Converter 2 waveforms when injecting positive voltage, (c) Converter 2 waveforms when injecting negative voltage

from Converter 2 as Converter 2 lowers down the load voltage to the nominal value of 288 V. The load voltage can be regulated continuously while the source voltage varies continuously so long as it is within the regulation range. The residual currents of I_{B2} at the beginning of the voltage regulation process and I_{B1} at the end, respectively, are the circulating current in the branch loop which is necessary to keep the voltage balance in the branch loop and the voltage between the two adjacent tap contacts. Fig. 4.15 (b) and Fig. 4.15 (c) are the zoom-in waveforms of Converter 2 voltage and current when the source is under-voltage and over-voltage, respectively. The different polarity of Converter 2 voltage and current indicates the opposite power flow directions of the converters under different voltage regulation conditions, where the branch current distribution also varies as seen from the upper branch current I_{B1}.

Based on the hardware test results, arcless tap change operation and load voltage regulation function are both verified. And the experimental performance matches the simulation results of the full-scale system. The power flow direction and current distribution correspond to the circuit analysis under different operation modes and conditions

Due to the partially rated power converter in the proposed topology, the efficiency impact to the conventional tap changer is much smaller compared to power electronic transformer and hybrid transformer. The scale-down prototype system's total efficiency is calculated by measuring the source and load active power for different voltage regulation conditions. The prototype's total efficiency is presented in Fig. 4.16. For the scale-down prototype of the conventional SVR, the measured efficiency is 97.2%. For the proposed hybrid voltage regulator, the prototype's highest total efficiency is 96.6%. As shown in Fig. 19, the maximum power loss due to the converters is 2.2% of the system's total power. Since both converters are industrial power assemblies where the switching devices are 1200V/100A IGBTs, the efficiency of the over-sized converter is relatively lower than the custom-designed converter.

The highest total efficiency is 96.6% when the source voltage is at 240V nominal voltage and no voltage regulation is required. As the source voltage deviates from the nominal voltage, a larger regulation voltage is injected and lower efficiency is observed. As the converters deliver more power at 220V and 260V source voltage, the converter efficiency becomes higher, but the absolute power loss of the converter becomes larger. Therefore, the total system efficiency becomes lower when the source voltage deviates from the 240V nominal voltage. It matches the total system efficiency analysis in Section IV which is based on the PLECS simulation results.

As shown in Table V, the converter is rated at 0.31% of the total system power in the full-scale medium voltage model. Considering the maximum converter power is 8.4% in the scale-down prototype due to lower input voltage, the medium voltage total system efficiency

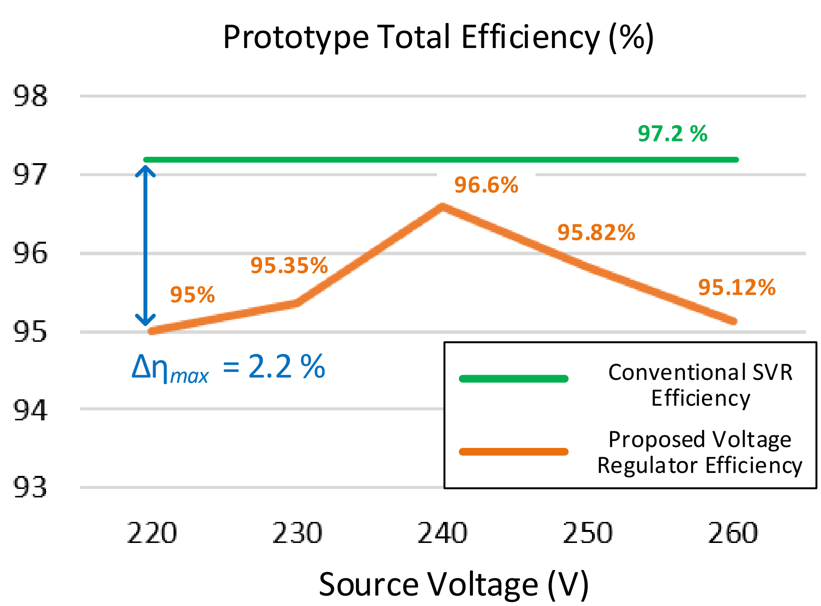

Figure 4.16 Measured prototype system efficiencies

can be much higher than the scale-down prototype. And most commercial low-frequency transformers present at least 98% efficiency. Since the maximum converter power loss is less than 0.04% of the total system power based on the full-scale model PLECS simulation results, the projected efficiency of the proposed hybrid voltage regulator in the medium voltage application is at least 97.96%.

To conclude, the proposed hybrid voltage regulator is a high-efficiency solution to achieve both arcless tap change and stepless voltage regulations. Longer operation lifetime, accurate voltage regulation, and high efficiency are the advantages of the proposed hybrid voltage regulator.

In this chapter, a hybrid voltage regulator based on conventional SVR and a fractionally rated (0.31%) power converter is proposed. The new device achieves both arcless tap change and stepless voltage regulation functions. Simulation and experimental results verify that the electric arc can be eliminated when tap changes. This reduces the contact erosion rate by 1055 times and significantly extends the lifetime of the voltage regulator. Fast and accurate voltage regulations are also guaranteed by the proposed hybrid voltage regulator. Both functions are achieved by a back-to-back power converter with different control strategies, which are validated by the scaled-down experimental results. The power converter capacity of the proposed solution in the full-scale distribution system is only 0.31% of the distribution transformer power rating, which significantly reduces the additional power converter cost and achieves a high system efficiency in the medium voltage applications. The proposed solution requires minimal changes to the existing SVR, but eliminates the arcing nature of these tap changers and achieves accurate and stepless load voltage regulation. The proposed solution will significantly enhance the reliability and lifetime of the voltage regulators, meanwhile, improve the voltage fluctuations in the distribution system due to renewable integrations.

CHAPTER 5: HYBRID TRANSFORMER BASED ON INTERLINE POWER CONVERTERS

The hybrid transformer is mostly used for voltage regulation and var control with a fractionally rated power converter, which reduces the device cost and increases the overall efficiency compared with the Solid State Transformer (SST). Conventionally, the voltage is compensated by injecting voltage in series with the load. This paper proposed a new hybrid transformer based on interline power converters for voltage regulation. The maximum power delivered by converters is reduced in half compared with the conventional series compensation configuration for the same voltage regulation range. Therefore, the proposed hybrid transformer exhibits a higher overall efficiency covering a wide range of voltage regulation. Comparison between the conventional series voltage compensation method and the proposed interline power converter-based method is presented based on the operation principle, the converter power, and the overall system efficiency.

In power distribution systems, distribution transformers are widely applied to provide isolation between different voltage levels. The voltage drop across distribution lines and power delivery variation can be frequently observed in distribution systems. Therefore, some voltage regulation devices are implemented to regulate the load voltage. Step voltage regulator (SVR) has been utilized in power distribution systems for decades to regulate the voltage step by step while the voltage regulation speed is limited by the tap changer mechanism. In recent years, voltage variation can be observed more frequently due to renewable energy penetration and the power generation variation from distributed energy resource (DER). Arcless tap change technologies and other accurate voltage regulation methods are discussed in previous chapters. However, distribution transformers are expected to achieve fast voltage regulation with cost-efficient solutions. Dynamic voltage restorer (DVR) at medium voltage level is to compensate voltage sag and swell for transient voltage variation. Solid-state transformer is an advanced technology rated at the feeder's full power. Hybrid transformer solutions present the advantages of high efficiency and low cost. The distributed var control is also available for the hybrid distribution transformer. The controllable network transformer in [42] and the interline power flow controller in [43] provide new configurations for voltage regulation.

5.1 Proposed Hybrid Transformer Based on Interline Power Converters

The configuration of the proposed hybrid transformer is shown in Fig. 5.1. An additional winding which is placed in series with the secondary winding covers the complete load voltage regulation range. Two series transformers are connected in series with top and bottom branches, respectively. An interline back-to-back power converter

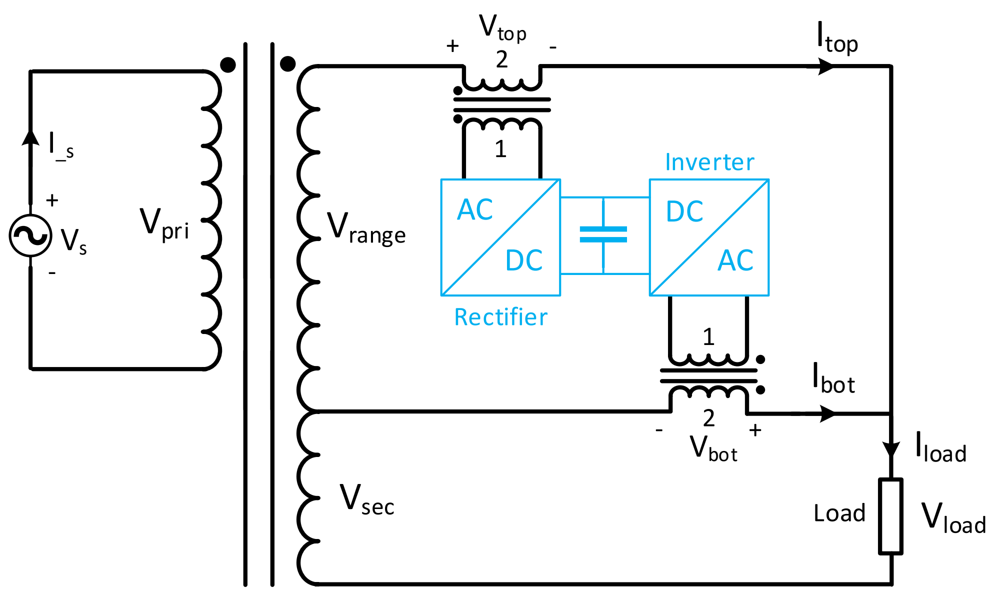

Figure 5.1 Proposed hybrid transformer

connects two series transformers in the middle. The converter regulates the DC bus voltage while the inverter controls the bottom winding voltage V_{bot}, so the load voltage can be regulated and the top winding voltage V_{top} changes accordingly. The load voltage can be expressed by equation (40) and the nominal load voltage, as equation (41), is acquired when V_{top} and V_{bot} are both half of the additional winding voltage V_{range}. Equation (42) and (43) show the current and voltage distribution relationships in the top and bottom branches where I_{top} and I_{bot} are top and bottom branch current respectively. Rectifier power P_{rec} and inverter power P_{inv} can be calculated by equation (44).

$$V_{load} = V_{sec} + V_{bot} \tag{40}$$

$$V_{load(nominal)} = V_{sec} + 0.5\,V_{range} \tag{41}$$

$$I_{top} + I_{bot} = I_{load} \tag{42}$$

$$V_{range} = V_{top} + V_{bot} \tag{43}$$

$$P_{rec} = V_{top} I_{top} = P_{inv} = V_{bot} I_{bot} \tag{44}$$

For the same voltage variation between $\pm\Delta V$ from the source, the top and bottom branch voltage and current curves are illustrated in Fig. 5.2. As the regulation voltage

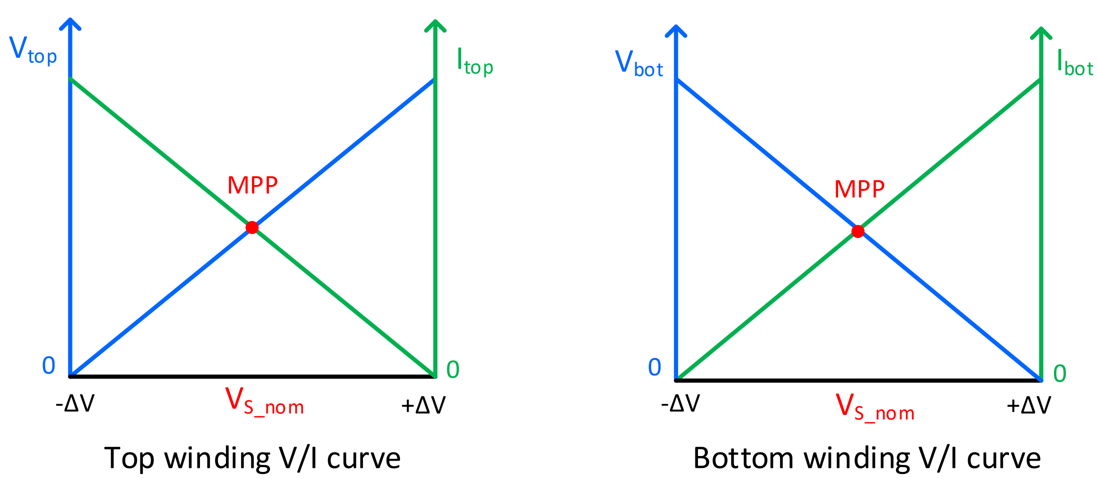

Figure 5.2 Top and bottom winding V/I curve (MPP: maximum power point)

changes from $-\Delta V$ to $+\Delta V$, the branch winding voltage and current change with different slopes. However, for the conventional series voltage compensation strategy, the series transformer winding current is constant as the load current but the series winding voltage varies linearly with the regulation voltage ΔV.

5.2 Comparison Between The Proposed and The Conventional Methods

To compare the proposed hybrid transformer and the conventional hybrid transformer based on series voltage compensation, a reference distribution load model is provided in Table VII. To simplify the model, an 80-kW resistive load is used for both transformer models. Both systems target on 10% load voltage regulation range for the 4 kV/20 A nominal loading condition. Based on the same reference load model, the hybrid transformer parameters of the two solutions are listed in Table VIII and Table IX. For the conventional series regulation solution, the maximum converter power is proportional to

Table VII REFERENCE LOAD MODEL SPECIFICATIONS

Parameter	**Value**
Source voltage	4 kV
Nominal load voltage	4 kV
Load current	20 A
Resistive load power	80 kW
Voltage regulation range	±400 V
Voltage regulation percentage	±10%

$$P_{series(max)} = \Delta V \cdot I_{load} \tag{45}$$

$$V_{range} = 2 \cdot \Delta V \tag{46}$$

$$\begin{aligned} P_{interline(max)} &= 0.5 V_{range} \cdot 0.5 I_{load} \\ &= 0.5 P_{series(max)} \end{aligned} \tag{47}$$

Table VIII PROPOSED HYBRID TRANSFORMER SPECIFICATIONS

Parameter	Value
Primary winding voltage V_{pri}	4 kV
Secondary winding voltage V_{sec}	3.6 kV
Additional winding voltage V_{range}	800 V
Nominal branch current I_{top}/ I_{bot}	10 A
Nominal branch voltage V_{top}/ V_{bot}	400 V
Maximum converter power	4 kW
DC bus voltage	800 V
Series transformer turns ratio (N)	1:2
Converter switching frequency	10 kHz

the voltage regulation range. Specifically, 10% converter power is required for 10% load voltage regulation range. In the proposed interline-based hybrid transformer, it is noted that the additional winding voltage V_{range} needs to cover the entire voltage regulation range of 800 V while the nominal branch current is just half of the load current. Based on equation

Table IX CONVENTIONAL SERIES HYBRID TRANSFORMER SPECIFICATIONS

Parameter	Value
Primary winding voltage V_{pri}	4 kV
Secondary winding voltage V_{sec}	4 kV
Nominal load current I_{load}	20 A
Regulation voltage range ΔV	400 V
Maximum converter power	8 kW
DC bus voltage	800 V
Series transformer turns ratio (N)	1:1
Converter switching frequency	10 kHz

(45)-(47), the maximum converter power of the interline hybrid solution is 4 kW which is half of the maximum converter power in the conventional series solution.

For the conventional series solution, the rectifier is connected with a shunt winding on the main transformer and only provides power for the inverter to regulate the load voltage. However, for the proposed interline solution, the rectifier participates in the top branch voltage control as well to change the voltage distribution in the top and bottom branch loop, which contributes to the lower maximum converter power and the higher overall transformer efficiency.

5.3 Simulation Results

The proposed hybrid transformer based on interline power converters is developed in MATLAB Simulink to verify the operation principles. The system parameters are the same as in Table VII and Table VIII. Rectifier and inverter are both H-bridge configuration. In the simulation, the load voltage close-loop control is implemented. The simulation results are shown in Fig. 5.3. From 1s to 2s, the source voltage increases from 3.6 kV to 4 kV, and the load voltage is regulated to 4 kVrms nominal voltage. The top winding voltage increases while its current decreases. On the contrary, the bottom winding voltage and current change in a reverse pattern. Meanwhile, the total of the top and bottom winding voltages is the same with the regulation range voltage V_{range}. The total of the top and bottom winding currents equals the load current. Equations from the previous analysis are verified by the simulation results. The voltage and current changes in the simulation results match the previous model analysis in Fig. 5.2. The operation principles are verified by the simulation results.

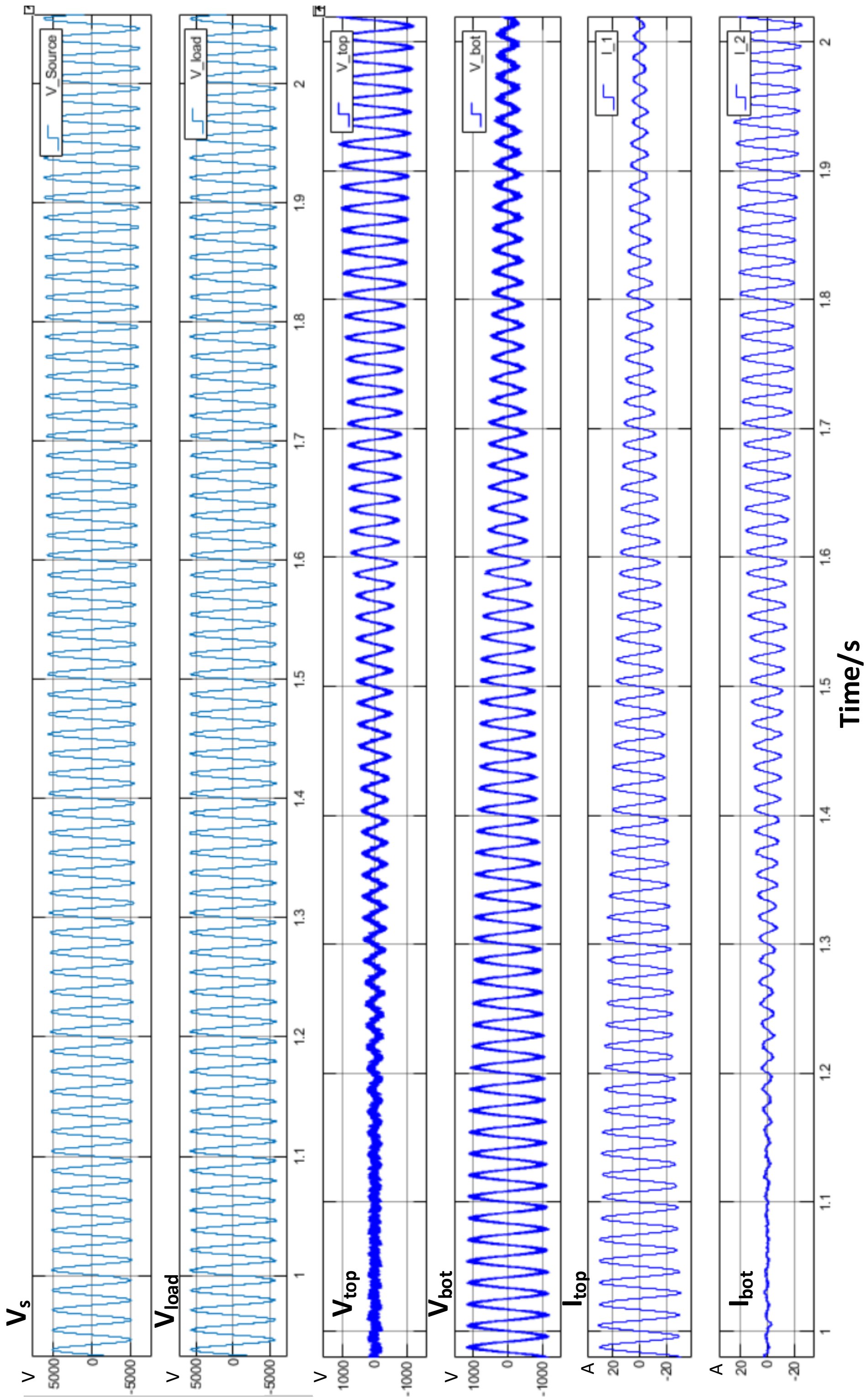

Figure 5.3 Voltage regulation waveforms of the proposed hybrid transformer. (From top to bottom: source voltage, load voltage, top winding voltage, bottom winding voltage, top branch current and bottom winding current.)

5.4 Converter Power Loss and Overall Efficiency Comparison

To further investigate the converter power loss and the transformer overall efficiency, simulation models of the conventional series solution and the proposed interline solution are developed in PLECS. The transformers are ideal in the simulation. Based on the converter ratings, Infineon IGBT IGW60T120 rated at 1200V and 60A is selected as the switching devices in the converter. The operation temperature is 70 degrees Celsius.

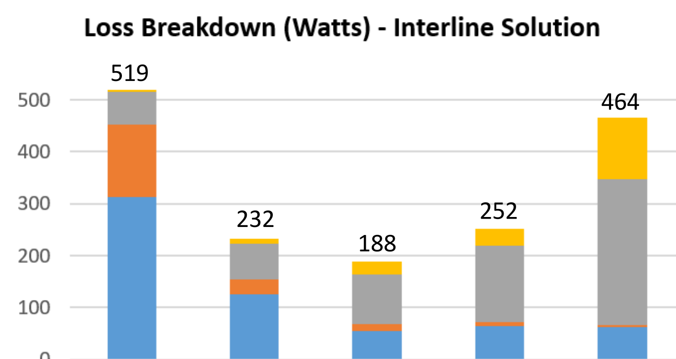

Source Voltage	3.6kV	3.8kV	4 kV	4.2 kV	4.4 kV
Inv Cond. Loss	3.48	9.93	24.97	33.51	118.02
Inv Sw. Loss	63.52	67.54	94.64	147.38	281.17
Rec Cond. Loss	138.68	30.01	13.27	7.29	2.74
Rec Sw. Loss	313.46	124.88	55.47	64.07	63

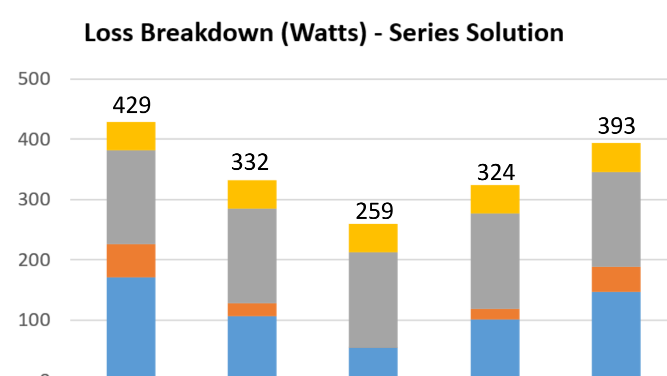

Source Voltage	3.6kV	3.8kV	4 kV	4.2 kV	4.4 kV
Inv Cond. Loss	46.73	47.07	47.36	47.65	47.92
Inv Sw. Loss	156.88	157.5	157.38	157.47	158.02
Rec Cond. Loss	55.02	20.97	1.01	17.69	40.87
Rec Sw. Loss	170.17	106.37	53.4	101.37	146.74

Figure 5.4 Converter loss breakdown. (Up: proposed interline solution, down: conventional series solution.)

The converter total power loss and the loss breakdown are shown in Fig. 5.4 based on different source voltage while the load voltage is regulated to 4 kV. It is observed that the rectifier and inverter switching loss and conduction loss are highly related to the current flowing through the converter. Therefore, in the conventional series solution, the inverter power loss does not change much since the inverter current is constant as the load current while the rectifier power loss increases when the source voltage deviates from the nominal voltage. For the proposed interline solution, the rectifier loss decreases, and the inverter

Figure 5.5 Up: converter power comparison, down: transformer overall efficiency.

loss increases when the source voltage increases from 3.6 kV to 4 kV, which is also related to the top and bottom branch current distribution. It is noted that the absolute converter power loss of the proposed interline solution is lower than which of the conventional series solution across a wide range of the load voltage regulation, so the transformer overall efficiency of the interline solution is also higher than the series solution as shown in Fig. 5.5. Meanwhile, the maximum converter power of the interline solution is half of which of the conventional series solution.

5.5 Conclusion and Future Work

In this chapter, a new hybrid transformer based on interline power converters is proposed for voltage regulation. The operation principles are analyzed and validated by the simulation results. The proposed hybrid transformer presents a higher overall efficiency covering a wide range of voltage regulation and requires half maximum converter power compared with the conventional series voltage compensation configuration for the same voltage regulation range. For future work, a scale-down prototype will be developed to further verify the voltage regulation function and operation principles and a more detailed comparison between the two solutions will be included in the future.

CHAPTER 6: INVESTIGATION ON SERIES-CONNECTED VOLTAGE REGULATION TRANSFORMER

In modern power distribution systems, power electronics-based devices are expected to solve issues, such as fast voltage regulation, flicker compensation, and var control, which are not able to be achieved from the conventional step voltage regulators (SVR). This chapter proposed a new topology of the hybrid voltage regulation transformer (VRT). The feasibility and capability of var control are investigated for different load power factors and input voltage percentage when the voltage regulation does not exceed the power converter capacity. The simulation results illustrate the feasibility of implementing var control while the load voltage is being regulated. The var control implemented on the VRT can regulate the reactive power for each feeder in the distribution system in addition to the voltage regulation function.

6.1 Proposed Series-Connected Voltage Regulation Transformer

The configuration of the proposed VRT is shown in Fig. 6.1. The inverter injects regulation voltage in series from the primary side of the VRT through the upper and lower series transformers. Due to the special inverter output connection and series transformer polarity as shown in Fig. 6.1, the source current I_S is divided equally through the upper and lower paths as I_H and I_L, as shown in equation (48). With a shunt winding on the VRT supplying energy to the power converter, the series voltage regulation can be implemented constantly without energy limitation.

To analyze the voltage relationships, the upper and lower series transformer injected voltages are denoted as V_H and V_L. The series transformer turns ratio is N_t. The

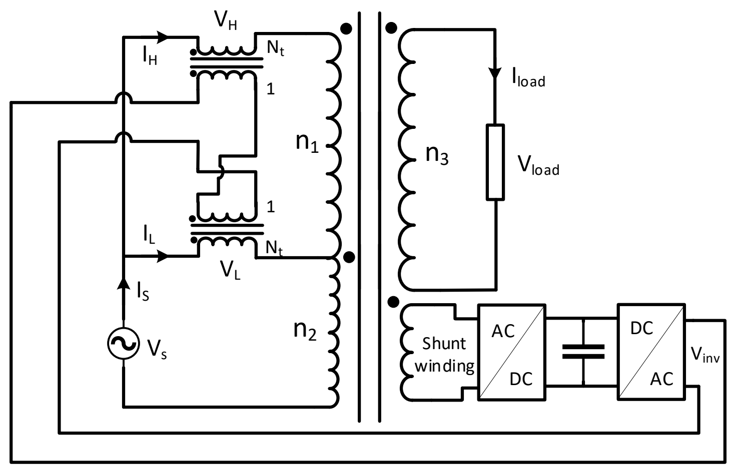

Figure 6.1 Proposed voltage regulation transformer

source voltage, load voltage, and inverter output voltages are V_S, V_L and V_{inv}, respectively. From the transformer winding flux linkage relationship, equation (49) can be derived and the load and source current relationship can be derived as equation (50). In the series transformer loop, the inverter output voltage multiplied by the series transformer turns ratio is the sum of V_H and V_L, as shown in equation (51). In equation (52), the load power is the sum of the source power and the inverter output power. By solving equation (48)-(52), the voltage relationships in the proposed VRT can be derived as equation (53).

$$I_H = I_L = 0.5\, I_S \tag{48}$$

$$0.5\, n_1 I_S + n_2 I_S = n_3 I_{load} \tag{49}$$

$$I_{load} = \frac{n_2 + 0.5 n_1}{n_3} I_S \tag{50}$$

$$V_H + V_L = N_t V_{inv} \tag{51}$$

$$V_{load} I_{load} = V_S I_S + 0.5 I_S (V_H + V_L) \tag{52}$$

$$V_{load} = \frac{n_3}{n_2 + 0.5 n_1} (V_s + 2V_{inv}) \tag{53}$$

6.2 Investigation on Var Control Capability

As the power converter regulates the voltage, there is also var control capability of the power converter if the converter's active power does not exceed the power capacity of the converter. The system parameters are listed in Table X. The power converter capacity and the voltage regulation range are rated at 10%. The var control capabilities and the limits are the focuses of the investigation besides the voltage regulation function. The benefit of var control from the power converter is that the power converter can share the reactive power control responsibilities of the conventional var control components in the distribution systems, such as STATCOM and other types of synchronous compensators. At the same time, the distributed var control can be implemented for each feeder in the distribution system.

Table X SIMULATION SPECIFICATIONS

Parameter	**Value**
Power rating	50 kVA
Source voltage	7200 V
Nominal load voltage	120 V
Load current	417 A
Converter capacity	5 kVA
Voltage regulation percentage	10 %
DC bus voltage	400 V
Series transformer turns ratio (N_t)	8:1
Converter switching frequency	10 kHz

Fig. 6.2 is the voltage regulation vector analysis for different loading conditions and voltage regulation angle conditions. The blue dashed circle is the target load voltage magnitude, while the brown dashed circle is the injected regulation voltage range. The intersections of the two circles mark the range of the regulated load voltage which can fall

on the dashed blue circle between the two intersections. V_{reg} is the injected regulation voltage. V' is the original load voltage at the VRT without voltage regulation. φ_L is the angle between V_{load} and I_{load} which is determined by the load power factor. φ_r is the angle between V_{load} and V' which is determined by the injected regulation voltage. The equations of the two dashed circles can be expressed as equation (54) and (55). By solving (54) and (55), the coordinates of two intersections are (56) and (57). The coordinates are the points where the maximum var control is obtained. The load active power and the active power provided by the source can be expressed as equation (58) and (59), respectively. With the exact coordinates of the maximum reactive power points, the angle φ_r can be calculated by equation (60). As the inverter injected active power is the difference of the source and load active power, as equation (61), the maximum reactive power can be expressed as equation (62). It is noted that the var control capability is doubled because the rectifier and inverter can both inject reactive power to the system shown in Fig. 6.1. The active power going

$$x^2 + y^2 = 120^2 \tag{54}$$

$$(x - V')^2 + y^2 = 12^2 \tag{55}$$

$$x = \frac{7128}{V\prime} + \frac{V\prime}{2} \tag{56}$$

$$y = V_q = \pm\sqrt{|120^2 - x^2|} \tag{57}$$

$$P_L = V_{load} I_{load} cos(\varphi_L) \tag{58}$$

$$P_s = V' I_{load} cos\,(\varphi_L - \varphi_r) \tag{59}$$

$$\varphi_r = sin^{-1}\left(\frac{y}{V_{load}}\right) = sin^{-1}\left(\frac{\pm\sqrt{\left|120^2 - \left(\frac{7128}{V\prime} + \frac{V\prime}{2}\right)^2\right|}}{V\prime}\right) \tag{60}$$

$$P_{inv} = P_L - P_s = V_{load} I_{load} cos\,(\varphi_L) - V' I_{load} cos\,(\varphi_L - \varphi_r) \tag{61}$$

$$Q_{max} = 2\sqrt{0.1S_{sys}^2 - P_{inv}^2} = 2\sqrt{0.1S_{sys}^2 - [V_{load} I_{load} cos\,(\varphi_L) - V' I_{load} cos\,(\varphi_L - \varphi_r)]^2} \tag{62}$$

through the rectifier and inverter is the same, hence the residual reactive power capacity is also the same for two converters.

Based on equation (62), the relationship between the maximum var control capability, load power factor and the input voltage percentage V_{in} can be plotted in MATLAB, as shown in Fig. 6.3. It can be observed that the var control capability range is the same when the power factor is 1. And the inductive load and capacitive load shows an opposite trend of the maximum var control range when the power factor is not unity.

For cases that the load voltage is only required to be regulated within a band limit, Fig. 6.4 gives an example of vector analysis when the load voltage is regulated within ±5% band limit. The shaded area in Fig. 6.4 is where the load voltage can be regulated. The

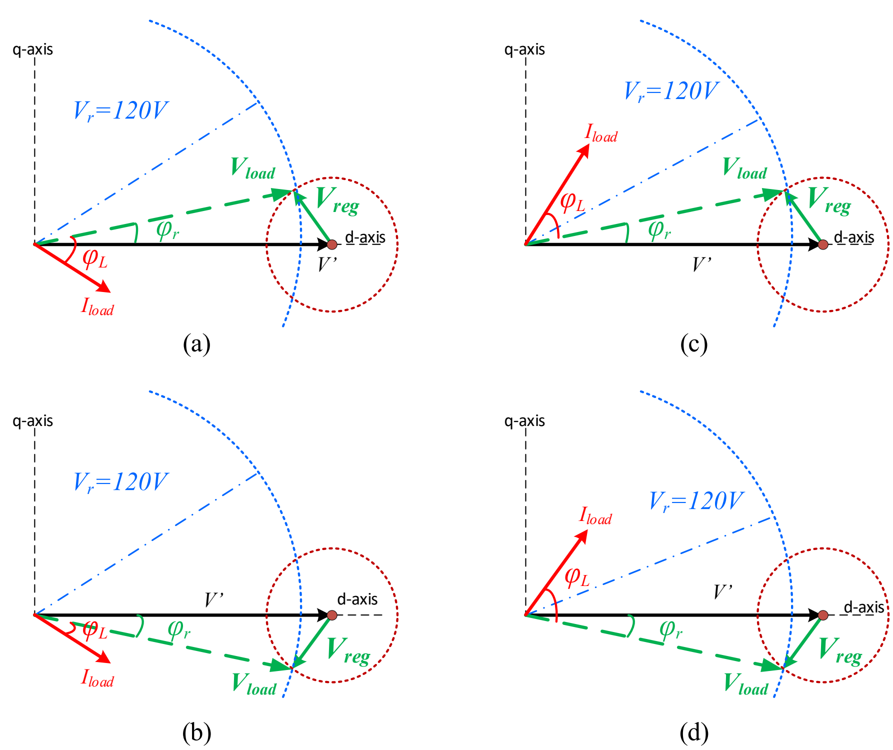

Figure 6.2 Voltage regulation vector analysis: (a) inductive load ($+\varphi_L$) leading regulation ($+\varphi_r$), (b) inductive load ($+\varphi_L$) lagging regulation ($-\varphi_r$), (c) capacitive load ($-\varphi_L$) leading regulation ($+\varphi_r$), (d) capacitive load ($-\varphi_L$) lagging regulation ($-\varphi_r$)

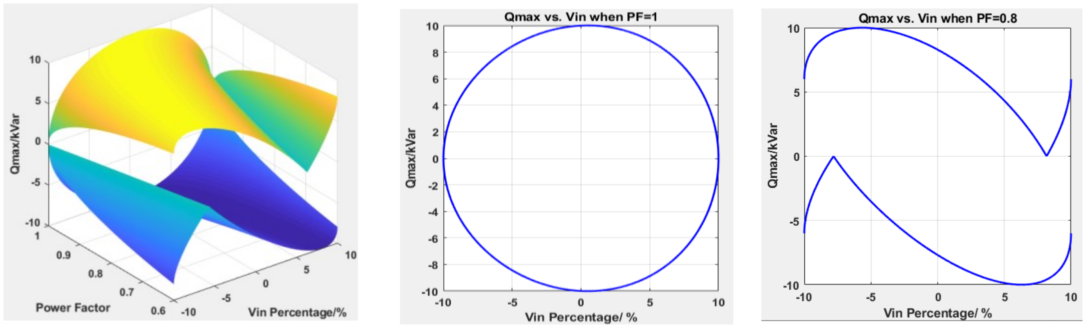

(a)

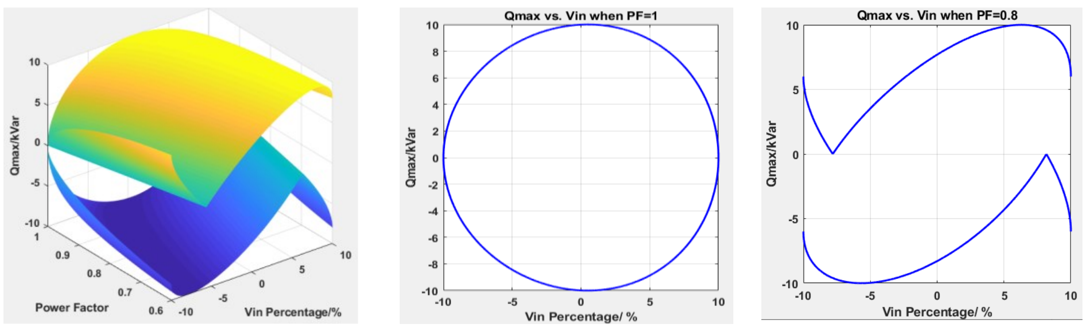

(b)

Figure 6.3 Var control capabilities for fixed load voltage magnitude (120V): (a) inductive load (+φ_L), (b) capacitive load (-φ_L)

maximum var control capabilities are illustrated in Fig. 6.5. It is indicated in Fig. 6.5 (c) that the converter can obtain maximum var control when V_{in} is within ±5% range.

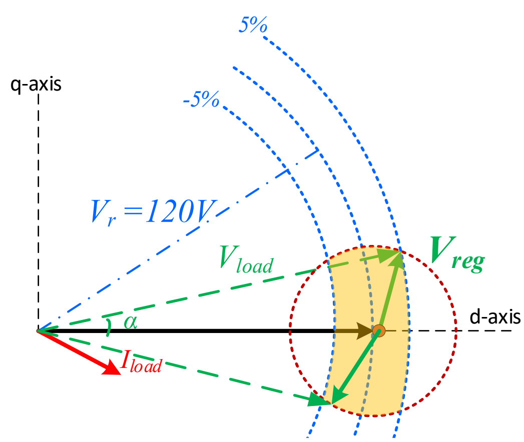

Figure 6.4 Voltage regulation with ±5% load voltage band limit

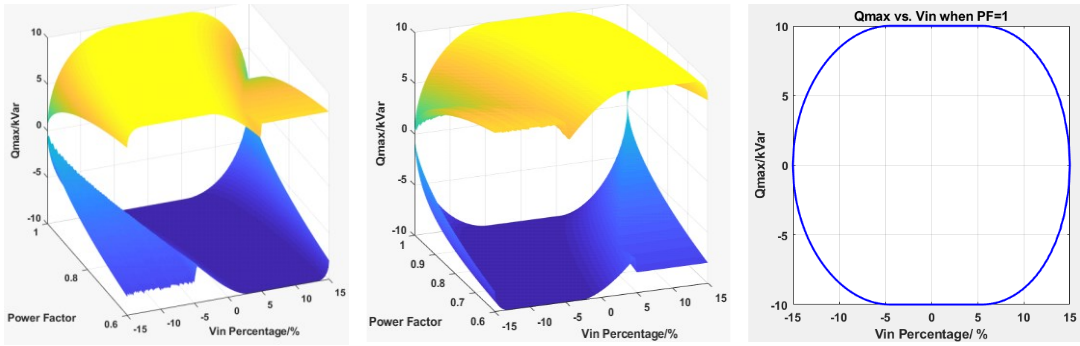

(a) (b) (c)

Figure 6.5 Var control capabilities: (a) inductive load, (b) capacitive load, (c) 2-D plot when power factor is 1

6.3 Simulation Results on Var Control Capability

Based on the proposed VRT in Fig. 6.1, a simulation model is developed to verify the previous analysis on the var control capability. The simulation condition is the same with the parameters listed in Table XI. As the source voltage changes, the voltage of the 50kW resistive load is regulated to 120 V and the power converter utilizes the residual capacity to achieve maximum var control points. In Fig. 6.6, the source voltage is at 7.2 kV rated value. The inverter maximum var control of 5 kVar is achieved from 1 to 1.5 s and the rectifier maximum var control of 5 kVar is achieved from 1.5 to 2 s. As a result, the power converter absorbs the reactive power from the source, which is 10 kVar in total.

In Fig. 6.7, the source voltage is at 7.92 kV which is the maximum rated voltage regulation of +10%. The load power is regulated to 50 kW while the power converter has no residual capacity for the var control. Therefore, the source reactive power is zero during the voltage regulation. The var control capacities when the source voltage is at 0 and +10% regulation correspond to the previous analysis in Fig. 6.3 when the load power factor is 1.

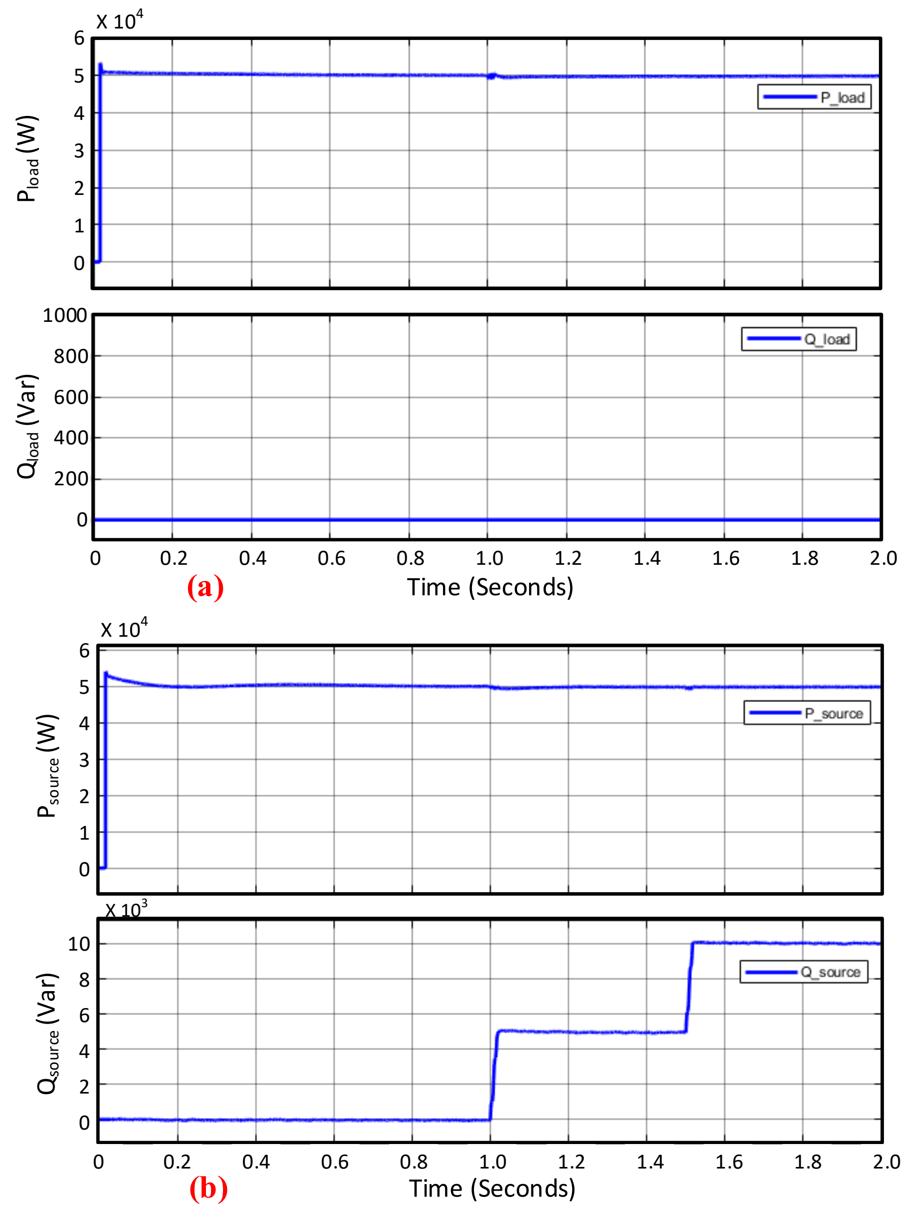

Figure 6.6 When V_{source} is at rated 7.2 kV, the active and reactive power of: (a) the load, (b) the source

In this chapter, a new voltage regulator topology is proposed for the hybrid voltage regulation transformer. The var control capabilities and limits for different input voltage percentage and load power factor are analyzed, which helps to fully understand the capability of the reactive power compensation for conventional voltage regulation devices. The simulation results validate the feasibility of implementing var control while the load

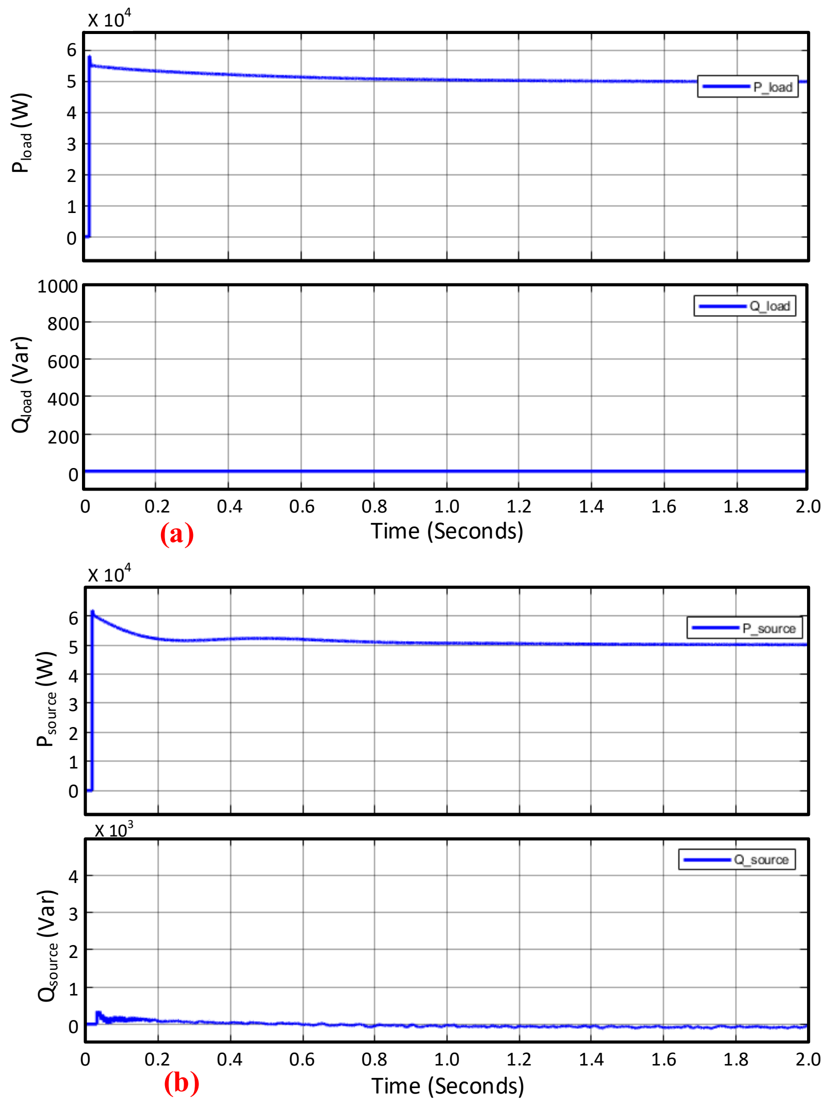

Figure 6.7 When V_{source} is at 7.92 kV (+10% variation), the active and reactive power of: (a) the load, (b) the source

voltage is being regulated. Var control capability of the VRT can expand the reactive power control capacity of the distribution system. The distributed var control from the VRT can relieve the stress of the conventional var control devices in the power distribution systems, such as STATCOM, Static Var Compensator.

CHAPTER 7: CONCLUSION AND FUTURE WORK

7.1 Publications

The following list is a summary of my main publications.

1. Y. Wang and T. Zhao, “A Hybrid Voltage Regulator with Arcless Tap Change and Stepless Voltage Regulation Functions,” *2020 IEEE Energy Conversion Congress and Exposition (ECCE)*, 2020, pp. 4857-4863, doi: 10.1109/ECCE44975.2020.9235339. [44]
2. Y. Wang, T. Zhao, M. Rashidi, J. Schaar and A. Trujillo, “An Arcless Step Voltage Regulator Based on Series-Connected Converter for Branch Current Suppression,” in IEEE Journal of Emerging and Selected Topics in Power Electronics, doi: 10.1109/JESTPE.2020.2989164. [45]
3. Y. Wang, X. Xu and T. Zhao, “An Arcless Step Voltage Regulator based on Paralleled Power Electronics Converter Configuration,” *2020 IEEE Applied Power Electronics Conference and Exposition (APEC)*, 2020, pp. 1006-1011, doi: 10.1109/APEC39645.2020.9124495. [46]
4. Y. Wang, X. Xu and T. Zhao, “An Arcless Voltage Regulator Based on Hybrid Tap Changing Topology,” *2018 9th IEEE International Symposium on Power Electronics for Distributed Generation Systems (PEDG)*, 2018, pp. 1-4, doi: 10.1109/PEDG.2018.8447789. [47]

7.2 Conclusion

This dissertation introduces the background of conventional step voltage regulators and the related issues with the conventional SVR. Challenges from the modern power distribution system are analyzed, such as arcing of tap change, voltage fluctuations, voltage sag and swell and voltage flickers. Based on the analysis, a technology roadmap of the proposed research work is presented to solve the related issues step by step. The literature review is also presented on the existing technologies for system-level solutions, arcless tap change methods, and PE-assisted voltage regulation. Multiple research works are conducted to solve the pre-existing issues. The main contributions are listed below.

- The proposed arcless voltage regulator can eliminate the arc by suppressing one target branch current before the mechanical tap changing movement. Arc comparison with the conventional SVR is also conducted based on the arc erosion rate. More practical functionalities, such as reactive power compensation and advanced load voltage regulation, are verified on the proposed arcless voltage regulator.
- The proposed arcless SVR integrates more functionalities, such as advanced load voltage regulation and volt/var control, in a single piece of equipment, so it shares the function of other similar devices, such as static synchronous compensators, in the existing distribution systems, which can eventually bring more flexibility to the planning and operation of the distribution system.
- A hybrid voltage regulator based on conventional SVR and a fractionally rated power converter is proposed. The new device achieves both arcless tap change and stepless voltage regulation functions.

- Arcless tap change operation reduces the contact erosion rate and significantly extends the lifetime of the voltage regulator. Fast and accurate voltage regulations are also guaranteed by the proposed hybrid voltage regulator. The power converter capacity of the proposed solution in the full-scale distribution system is only 0.31% of the distribution transformer power rating, which significantly reduces the additional power converter cost and achieves a high system efficiency in the medium voltage applications.
- The proposed solutions above require minimal changes to the existing SVR, but eliminates the arcing nature of these tap changers and achieves accurate and stepless load voltage regulation. The proposed solution will significantly enhance the reliability and lifetime of the voltage regulators, meanwhile improve the voltage fluctuations in the distribution system due to renewable integrations.
- A new hybrid transformer based on interline power converters is proposed for voltage regulation. The proposed hybrid transformer presents a higher overall efficiency covering a wide range of voltage regulation and requires half maximum converter power compared with the conventional series voltage compensation configuration for the same voltage regulation range.
- For the proposed voltage regulation transformer, the var control capabilities and limits for different input voltage percentage and load power factor are analyzed. Var control capability of the VRT can expand the reactive power control capacity of the distribution system. The distributed var control from the VRT

can relieve the stress of the conventional var control devices in the power distribution systems, such as STATCOM, Static Var Compensator.

7.3 Future Work

For future work, it can be addressed from two perspectives,

From the research and development perspective, the proposed voltage regulation transformer based on the interline topology needs to be further investigated. Hardware testing needs to be continued and completed for functional validation of voltage regulation and var control capabilities. In all proposed solutions and circuit configurations, the back-to-back power converter is an over-sized commercial power assembly. IGBT devices are over-qualified for the scale-down prototypes. Therefore, the design of power converters needs to be customized with the proper power rating, multi-level topologies, and wide-bandgap (WBG) switching devices, which will further reduce the power loss and efficiency impacts from the power converters [48] - [49]. Due to the existence of DC bus in the AC-DC-AC stages, all proposed topologies can be interconnected with local DC microgrids if necessary, which enables more different types of applications of the smart distribution transformers. Power flows are more flexible with local DC microgrids. Furthermore, local low-voltage DC loads can be supplied from the DC stage.

From the utility application perspective, the reliability and efficiency of the distribution transformer are always prior concerns. For the fractionally rated power converters, reliability enhancement and efficiency improvement are necessary for the proposed hybrid voltage regulator to be comparable to the conventional SVR. The reliability is not limited to the tap changer mechanism itself but is the reliability of holistic systems including the power converters. Other measures that actively monitoring the reliability and working status of the power converter are required. The proposed smart distribution transformers or voltage regulators should be investigated further at system levels since the smart transformers are capable of distributed advanced functions, such as flicker and sag/swell compensation, distributed var control, etc. Especially for the distributed var control capability, the stress of conventional var control devices, such as static var compensator (SVC) and STATCOM, will be relieved as var control can be implemented at multiple nodes where SVRs are located. The proposed hybrid voltage regulator and the proposed voltage regulation transformer are promising solutions to benefit the modern distribution systems in voltage regulation, var control and power flow control. The development of smart distribution transformers is as important as the development of Distributed Energy Resources (DERs), distributed power generation, and renewable energy technologies for modern power distribution systems.

REFERENCES

[1] X. Xu, Y. Wang and T. Zhao, "A Hybrid Switch based Arcless Voltage Regulator," *2018 9th IEEE International Symposium on Power Electronics for Distributed Generation Systems (PEDG)*, 2018, pp. 1-5, doi: 10.1109/PEDG.2018.8447868.

[2] R. Jongen, E. Gulski, K. Siodła, J. Parciak and J. Erbrink, "Diagnosis of degradation effects of on-load tap changer in power transformers," *2014 ICHVE International Conference on High Voltage Engineering and Application*, Poznan, 2014, pp. 1-4.

[3] J. J. Erbrink *et al*., "Diagnosis of Onload Tap Changer Contact Degradation by Dynamic Resistance Measurements," in *IEEE Transactions on Power Delivery*, vol. 25, no. 4, pp. 2121-2131, Oct. 2010.

[4] G. K. Ari and Y. Baghzouz, "Impact of high PV penetration on voltage regulation in electrical distribution systems," *2011 International Conference on Clean Electrical Power (ICCEP)*, Ischia, 2011, pp. 744-748.

[5] A. Hariri, M. O. Faruque, R. Soman and R. Meeker, "Impacts and interactions of voltage regulators on distribution networks with high PV penetration," *2015 North American Power Symposium (NAPS)*, Charlotte, NC, 2015, pp. 1-6.

[6] C. Roe, E. Farantatos, J. Meisel, A. P. Meliopoulos and T. Overbye, "Power System Level Impacts of PHEVs," *2009 42nd Hawaii International Conference on System Sciences*, Big Island, HI, 2009, pp. 1-10.

[7] A. D. Hilshey, P. D. H. Hines, P. Rezaei and J. R. Dowds, "Estimating the Impact of Electric Vehicle Smart Charging on Distribution Transformer Aging," in *IEEE Transactions on Smart Grid*, vol. 4, no. 2, pp. 905-913, June 2013.

[8] L. Cheng, Y. Chang and R. Huang, "Mitigating Voltage Problem in Distribution System with Distributed Solar Generation Using Electric Vehicles," in *IEEE Transactions on Sustainable Energy*, vol. 6, no. 4, pp. 1475-1484, Oct. 2015.

[9] D. Mao, J. Tan and J. Wang, "Location Planning of PEV Fast Charging Station: An Integrated Approach Under Traffic and Power Grid Requirements," in *IEEE Transactions on Intelligent Transportation Systems*, vol. 22, no. 1, pp. 483-492, Jan. 2021, doi: 10.1109/TITS.2020.3001086.

[10] D. Mao, D. Meyer and J. Wang, "Evaluating PEV's impact on long-term cost of grid assets," *2017 IEEE Power & Energy Society Innovative Smart Grid Technologies Conference (ISGT)*, 2017, pp. 1-5, doi: 10.1109/ISGT.2017.8086023.

[11] K. Kumar, S. Satsangi and G. B. Kumbhar, "Extension of life of distribution transformer using Volt-VAr optimisation in a distribution system," in *IET Generation, Transmission & Distribution*, vol. 13, no. 10, pp. 1777-1785, 21 5 2019, doi: 10.1049/iet-gtd.2018.5746.

[12] M. Kraiczy, T. Stetz and M. Braun, "Parallel Operation of Transformers With on Load Tap Changer and Photovoltaic Systems With Reactive Power Control," in *IEEE Transactions on Smart Grid*, vol. 9, no. 6, pp. 6419-6428, Nov. 2018, doi: 10.1109/TSG.2017.2712633.

[13] S. Akagi *et al.*, “Upgrading Voltage Control Method Based on Photovoltaic Penetration Rate,” in *IEEE Transactions on Smart Grid*, vol. 9, no. 5, pp. 3994-4003, Sept. 2018, doi: 10.1109/TSG.2016.2645706.

[14] G. L. Quinton, “Advantages of an Arcless Voltage Regulator,” in *IEEE Transactions on Industry Applications,* vol. IA-20, no. 2, pp. 425-428, March 1984.

[15] D. Dohnal and B. Kurth, “Vacuum switching, a well-proven technology has found its way into resistance-type load tap changers,” *2001 IEEE/PES Transmission and Distribution Conference and Exposition*, Atlanta, GA, 2001, vol.1, pp. 161-165.

[16] D. Monroy, A. Gomez-Exposito and E. Romero-Ramos, “Improving the voltage regulation of secondary feeders by applying solid-state tap changers to MV/LV transformers,” *2007 9th International Conference on Electrical Power Quality and Utilisation*, Barcelona, 2007, pp. 1-6.

[17] S. Martinez Garcia, J. C. Campo Rodriguez, J. A. Jardini, J. Vaquero Lopez, A. Ibarzabal Segura and P. M. MartÍnez Cid, “Feasibility of Electronic Tap-Changing Stabilizers for Medium Voltage Lines—Precedents and New Configurations,” in *IEEE Transactions on Power Delivery*, vol. 24, no. 3, pp. 1490-1503, July 2009.

[18] E. Martinez, I. Fernandez and J. M. Canales, “Thyristor based solid state tap changer for distribution transformers,” *2013 IEEE 11th International Workshop of Electronics, Control, Measurement, Signals and their application to Mechatronics*, Toulouse, 2013, pp. 1-5.

[19] J. Faiz and B. Siahkolah, “New solid-state on load tap-changers topology for distribution transformers,” in *IEEE Transactions on Power Delivery*, vol. 18, no. 1, pp. 136-141, Jan. 2003.

[20] J. de Oliveira Quevedo et al., “Analysis and Design of an Electronic On-Load Tap Changer Distribution Transformer for Automatic Voltage Regulation,” in *IEEE Transactions on Industrial Electronics*, vol. 64, no. 1, pp. 883-894, Jan. 2017.

[21] N. Chen and L. E. Jonsson, “A new Hybrid power electronics on-load tap changer for power transformer,” *2015 IEEE Applied Power Electronics Conference and Exposition (APEC)*, Charlotte, NC, 2015, pp. 1030-1037.

[22] G. R. Chandra Mouli, P. Bauer, T. Wijekoon, A. Panosyan and E. Bärthlein, “Design of a Power-Electronic-Assisted OLTC for Grid Voltage Regulation,” in *IEEE Transactions on Power Delivery*, vol. 30, no. 3, pp. 1086-1095, June 2015.

[23] D. J. Rogers and T. C. Green, “An Active-Shunt Diverter for On-load Tap Changers,” in *IEEE Transactions on Power Delivery*, vol. 28, no. 2, pp. 649-657, April 2013.

[24] C. van Schalkwyk, H. J. Beukes and H. du T Mouton, “An AC-to-AC converter-based voltage regulator,” *IEEE AFRICON. 6th Africon Conference in Africa,* George, South Africa, 2002, pp. 719-722 vol.2.

[25] R. Fourie and H. d. T. Mouton, “Development of a MV IGBT based solid-state tap changer,” *AFRICON 2009*, Nairobi, 2009, pp. 1-6.

[26] J. Kaniewski, P. Szczesniak, M. Jarnut and G. Benysek, “Hybrid Voltage Sag/Swell Compensators: A Review of Hybrid AC/AC Converters,” in IEEE Industrial Electronics Magazine, vol. 9, no. 4, pp. 37-48, Dec. 2015.

[27] C. Kumar and M. Liserre, “Operation and control of smart transformer for improving performance of medium voltage power distribution system,” 2015 IEEE 6th International Symposium on Power Electronics for Distributed Generation Systems (PEDG), Aachen, 2015, pp. 1-6

[28] H. Lee and Y. Yoon, “Intelligent Transformer Unit Topology Using Additional Small Power Converter Based on Conventional Distribution Transformer,” *2019 IEEE Energy Conversion Congress and Exposition (ECCE)*, Baltimore, MD, USA, 2019, pp. 4639-4645, doi: 10.1109/ECCE.2019.8912672.

[29] R. Ekström, K. Thomas and M. Leijon, “Fast solid-state on-load tap change using two current-controlled voltage-source inverters,” in *IET Power Electronics*, vol. 7, no. 10, pp. 2610-2617, 10 2014.

[30] J. E. Huber and J. W. Kolar, “Applicability of Solid-State Transformers in Today’s and Future Distribution Grids,” in *IEEE Transactions on Smart Grid*, vol. 10, no. 1, pp. 317-326, Jan. 2019.

[31] X. She, A. Q. Huang and R. Burgos, “Review of Solid-State Transformer Technologies and Their Application in Power Distribution Systems,” in *IEEE Journal of Emerging and Selected Topics in Power Electronics*, vol. 1, no. 3, pp. 186-198, Sept. 2013, doi: 10.1109/JESTPE.2013.2277917.

[32] J. G. Nielsen, M. Newman, H. Nielsen and F. Blaabjerg, “Control and testing of a dynamic voltage restorer (DVR) at medium voltage level,” in *IEEE Transactions on Power Electronics*, vol. 19, no. 3, pp. 806-813, May 2004, doi: 10.1109/TPEL.2004.826504.

[33] M. J. Newman, D. G. Holmes, J. G. Nielsen and F. Blaabjerg, “A dynamic voltage restorer (DVR) with selective harmonic compensation at medium voltage level,” in *IEEE Transactions on Industry Applications*, vol. 41, no. 6, pp. 1744-1753, Nov.-Dec. 2005, doi: 10.1109/TIA.2005.858212.

[34] Y. W. Li, D. M. Vilathgamuwa, P. C. Loh and F. Blaabjerg, “A Dual-Functional Medium Voltage Level DVR to Limit Downstream Fault Currents,” in *IEEE Transactions on Power Electronics*, vol. 22, no. 4, pp. 1330-1340, July 2007, doi: 10.1109/TPEL.2007.900589.

[35] Z. Shuai, P. Yao, Z. J. Shen, C. Tu, F. Jiang and Y. Cheng, “Design Considerations of a Fault Current Limiting Dynamic Voltage Restorer (FCL-DVR),” in *IEEE Transactions on Smart Grid*, vol. 6, no. 1, pp. 14-25, Jan. 2015, doi: 10.1109/TSG.2014.2357260.

[36] V. Verma and R. Gour, “Step-less voltage regulation on radial feeder with OLTC transformer-DVR hybrid,” *2015 6th International Conference on Power Electronics Systems and Applications (PESA)*, Hong Kong, 2015, pp. 1-6, doi: 10.1109/PESA.2015.7398912.

[37] C. Wang, X. Yin, Z. Zhang and M. Wen, “A Novel Compensation Technology of Static Synchronous Compensator Integrated with Distribution Transformer,” in *IEEE Transactions on Power Delivery*, vol. 28, no. 2, pp. 1032-1039, April 2013, doi: 10.1109/TPWRD.2012.2237526.

[38] L. Wang, C. Lam and M. Wong, “A Hybrid-STATCOM With Wide Compensation Range and Low DC-Link Voltage,” in *IEEE Transactions on Industrial Electronics*, vol. 63, no. 6, pp. 3333-3343, June 2016, doi: 10.1109/TIE.2016.2523922.

[39] M. A. Radi and M. Darwish, “Var control considerations for the design of hybrid distribution transformers,” *11th IET International Conference on AC and DC Power Transmission*, Birmingham, 2015, pp. 1-9, doi: 10.1049/cp.2015.0071.

[40] P. G. Slade, *Electrical Contacts: Principles and Applications*, United States: CRC Press, 1999

[41] *Datasheet IKQ120N60T*, Infineon Technologies, Neubiberg, Germany, 1999-2021. [Online]. Available: https://www.infineon.com/dgdl/Infineon-IKQ120N60T-DS-v02_03-EN.pdf?fileId=5546d46249cd10140149d230bd094df7

[42] D. Das, D. M. Divan and R. G. Harley, “Power flow control in networks using controllable network transformers,” in *IEEE Transactions on Power Electronics*, vol. 25, no. 7, pp. 1753-1760, July 2010, doi: 10.1109/TPEL.2010.2042076.

[43] Y. Zhang, Y. Zhang and C. Chen, “A Novel Power Injection Model of IPFC for Power Flow Analysis Inclusive of Practical Constraints,” in *IEEE Transactions on Power Systems*, vol. 21, no. 4, pp. 1550-1556, Nov. 2006, doi: 10.1109/TPWRS.2006.882458.

[44] Y. Wang and T. Zhao, “A Hybrid Voltage Regulator with Arcless Tap Change and Stepless Voltage Regulation Functions,” *2020 IEEE Energy Conversion Congress and Exposition (ECCE)*, 2020, pp. 4857-4863, doi: 10.1109/ECCE44975.2020.9235339.

[45] Y. Wang, T. Zhao, M. Rashidi, J. Schaar and A. Trujillo, “An Arcless Step Voltage Regulator Based on Series-Connected Converter for Branch Current Suppression,” in *IEEE Journal of Emerging and Selected Topics in Power Electronics*, doi: 10.1109/JESTPE.2020.2989164.

[46] Y. Wang, X. Xu and T. Zhao, “An Arcless Step Voltage Regulator based on Paralleled Power Electronics Converter Configuration,” *2020 IEEE Applied Power Electronics Conference and Exposition (APEC)*, 2020, pp. 1006-1011, doi: 10.1109/APEC39645.2020.9124495.

[47] Y. Wang, X. Xu and T. Zhao, “An Arcless Voltage Regulator Based on Hybrid Tap Changing Topology,” *2018 9th IEEE International Symposium on Power Electronics for Distributed Generation Systems (PEDG)*, 2018, pp. 1-4, doi: 10.1109/PEDG.2018.8447789.

[48] Z. Wang, Y. Wu, M. H. Mahmud, Z. Zhao, Y. Zhao and H. A. Mantooth, “Design and Validation of A 250-kW All-Silicon Carbide High-Density Three-Level T-Type Inverter,” in *IEEE Journal of Emerging and Selected Topics in Power Electronics*, vol. 8, no. 1, pp. 578-588, March 2020, doi: 10.1109/JESTPE.2019.2951625.

[49] H. Liu, T. Zhao and X. Wu, “Efficiency Improvement Evaluation and Loss Modeling of a Hybrid Switch-Based T-NPC Inverter,” *2019 IEEE 7th Workshop on Wide Bandgap Power Devices and Applications (WiPDA)*, 2019, pp. 6-11, doi: 10.1109/WiPDA46397.2019.8998807.